

# The Nucleon Anapole Moment and Parity-Violating $ep$ Scattering

Shi-Lin Zhu<sup>a</sup>, S.J. Puglia<sup>a</sup>, B.R. Holstein<sup>c</sup>, M. J. Ramsey-Musolf<sup>a,b</sup>

<sup>a</sup> Department of Physics, University of Connecticut, Storrs, CT 06269 USA

<sup>b</sup> Theory Group, Thomas Jefferson National Laboratory, Newport News, VA 23606 USA

<sup>c</sup> Department of Physics and Astronomy, University of Massachusetts, Amherst, MA 01003 USA

## Abstract

Parity-violating (PV) interactions among quarks in the nucleon induce a PV  $\gamma NN$  coupling, or anapole moment (AM). We compute electroweak gauge-independent contributions to the AM through  $\mathcal{O}(1/\Lambda_\chi^2)$  in chiral perturbation theory. We estimate short-distance PV effects using resonance saturation. The AM contributions to PV electron-proton scattering slightly enhance the axial vector radiative corrections,  $R_A^p$ , over the scale implied by the Standard Model when weak quark-quark interactions are neglected. We estimate the theoretical uncertainty associated with the AM contributions to  $R_A^p$  to be large, and discuss the implications for the interpretation PV of  $ep$  scattering.

PACS Indices: 21.30.+y, 13.40.Ks, 13.88.+e, 11.30.Er

## I. INTRODUCTION

The SAMPLE collaboration at MIT-Bates has recently reported a value for the strange-quark magnetic form factor measured using backward angle parity-violating (PV) electron-proton scattering [1]:

$$G_M^{(s)}(Q^2 = 0.1 \text{ GeV}^2/c^2) = 0.61 \pm 0.27 \pm 0.19 \quad , \quad (1)$$

where the first error is experimental and the second is theoretical. The dominant contribution to the theoretical error is uncertainty associated with radiative corrections to the axial vector term in the backward angle left-right asymmetry  $A_{LR}$  [2]:

$$A_{LR} \propto Q_W^P + Q_W^N \frac{G_M^n}{G_M^p} + Q_W^{(0)} \frac{G_M^{(s)}}{G_M^p} - (1 - 4\sin^2 \theta_W) \sqrt{1 + 1/\tau} \frac{G_A^p}{G_M^p} \quad , \quad (2)$$

where  $Q_W^P$  and  $Q_W^N$  are the proton and neutron weak charges, respectively,  $Q_W^{(0)}$  is the SU(3)-singlet weak charge\*,  $\theta_W$  is the weak mixing angle, and  $\tau = Q^2/4M_n^2$ . The axial form factor is normalized at the photon point as

$$G_A^p(0) = -g_A[1 + R_A^p] \quad (3)$$

where  $g_A = 1.267 \pm 0.004$  [3] is the nucleon's axial charge as measured in neutron  $\beta$ -decay and  $R_A^p$  denotes process-dependent electroweak radiative corrections to the  $V(e) \times A(p)$  scattering amplitude.

The radiative correction  $R_A^p$  is the subject of the present study. It was first analyzed in Ref. [4] and found to be large, negative in sign, and plagued by considerable theoretical uncertainty. Generally,  $R_A^p$  contains two classes of contributions. The first involve electroweak radiative corrections to the elementary  $V(e) \times A(q)$  amplitudes, where  $q$  is any one of the quarks in the proton. These radiative corrections, referred to henceforth as “one-quark” radiative corrections, are calculable in the Standard Model. They contain little theoretical uncertainty apart from the gentle variation with Higgs mass and long-distance QCD effects involving light-quark loops in the  $Z - \gamma$  mixing tensor. The one-quark contributions can be large, due to the absence from loops of the small  $(1 - 4\sin^2 \theta_W)$  factor appearing at tree level (see Eq. (2)) and the presence of large logarithms of the type  $\ln(m_q/M_Z)$ .

A second class of radiative corrections, which we refer to as “many-quark” corrections, involve weak interactions among quarks in the proton. In this paper, we focus on those many-quark corrections which generate an axial vector coupling of the photon to the proton (see Figure 1). This axial vector  $pp\gamma$  interaction, also known as the anapole moment (AM), has the form

---

\*Note that in Ref. [2], the weak charges are denoted  $\xi_V^{p,n,(0)}$ .

$$\mathcal{L}^{AM} = \frac{e}{\Lambda_\chi^2} \bar{N} (a_s + a_v \tau_3) \gamma_\mu \gamma_5 N \partial_\nu F^{\nu\mu} . \quad (4)$$

(Here, we have elected to normalize the interaction to the scale of chiral symmetry breaking,  $\Lambda_\chi = 4\pi F_\pi$ .) These many-quark anapole contributions to  $R_A^p$ , which are independent of the electroweak gauge parameter [5], were first studied in Ref. [4] and found to carry significant theoretical uncertainty. The scale of this uncertainty was estimated in Ref. [4], and this value was used to obtain the theoretical error in Eq. (1).

In order to better constrain the error in  $G_M^{(s)}$  associated with  $R_A^p$ , the SAMPLE collaboration performed a second backward angle PV measurement using quasielastic (QE) scattering from the deuteron. The asymmetry  $A_{LR}(\text{QE})$  is significantly less sensitive to  $G_M^{(s)}$  than is  $A_{LR}(ep)$ , but retains a strong dependence on  $R_A^{T=1}$ , the *isovector* part of  $R_A^p$ . The calculation of Ref. [4] found the uncertainty in  $R_A^p$  to be dominated by this isovector component— $R_A^{T=1} \approx -0.34 \pm 0.20$ —and the goal of the deuterium measurement was, therefore, to constrain the size of this largest term. A preliminary deuterium result was reported at the recent Bates25 Symposium at MIT, and suggests that  $R_A^{T=1}$  has the same negative sign as computed in Ref. [4] but has considerably larger magnitude, possibly of order unity [6]. Combining this result with the previous  $A_{LR}(ep)$  measurement would yield a nearly vanishing value for  $G_M^{(s)}$ , rather than the large and positive value quoted in Eq. (1).

The prospective SAMPLE result for  $R_A^{T=1}$  is remarkable, indicating that a higher-order electroweak radiative correction is of the same magnitude as, and cancels against, the tree-level amplitude! The occurrence of such enhanced electroweak radiative corrections is rare. Nevertheless, there does exist at least one other instance in which higher-order electroweak processes can dominate the axial vector hadronic response, namely, the nuclear anapole moment. The anapole moment of a heavy nucleus grows as  $A^{2/3}$  (see, *e.g.* Refs. [5,7] and references therein). Because of the scaling with mass number, the nuclear AM contribution to a  $V(e) \times A(\text{nucleus})$  amplitude can be considerably larger than the corresponding tree-level  $Z^0$ -exchange amplitude, and this  $A^{2/3}$  enhancement is consistent with the size of the Cesium AM recently determined by the Boulder group using atomic parity-violation [8]. The reason behind the enhancement of  $R_A^{T=1}$  for the few-nucleon system, however, is *not* understood. The goal of the present paper is to investigate whether there exist conventional, hadronic physics effects which can explain the enhancement apparently implied by the SAMPLE deuterium measurement.

In order to address this question, we revisit the analysis of Ref. [4]. Following Ref. [9], we re-cast that analysis into the framework of heavy baryon chiral perturbation theory (HBChPT) [10,11]. We carry out a complete calculation of  $R_A^{T=1}$  and  $R_A^{T=0}$  to order  $1/\Lambda_\chi^2$ , including loop diagrams not considered in Refs. [4,9]. We also extend those analyses to include decuplet as well as octet intermediate states, magnetic insertions, and SU(3) chiral symmetry. As in Ref. [4], we estimate the chiral counterterms at  $\mathcal{O}(1/\Lambda_\chi^2)$  using vector meson saturation. However, we go beyond that previous analysis and determine the sign of this vector meson contribution phenomenologically. We find that decuplet intermediate states and magnetic insertions do not contribute up to the chiral order at which we truncate. Also, the effect of SU(3) symmetry, in the guise of kaon loops, is

generally smaller than the pion loops considered previously. In the end, we express our results in terms of effective PV hadronic couplings. Some of these couplings may be determined from nuclear and hadronic PV experiments or detailed calculations (for reviews, see Refs. [12,13]), while others are presently unconstrained by measurement. Guided by phenomenology and the dimensional analysis of Ref. [9], we estimate the range of possible values for the new couplings. We suspect that our estimates are overly generous. Nevertheless, we find that – even under liberal assumptions – the AM contributions to  $R_A^{T=1}$  appear unable to enhance the one-quark corrections to the level apparently observed by the SAMPLE collaboration and, in our conclusions, we speculate on possible additional sources of enhancement not considered here.

The remainder of the paper is organized as follows. In Section 2, we relate the anapole couplings  $a_{s,v}$  to the radiative corrections,  $R_A^{T=0,1}$ , and in Section 3, we outline our formalism for computing these couplings in HBChPT. A reader already familiar with this formalism may wish to skip to Section 4, where we compute the chiral loop contributions to the nucleon anapole moment through  $\mathcal{O}(1/\Lambda_\chi^2)$ . We also include the leading  $1/m_N$  terms in the heavy baryon expansion, which generate contributions of  $\mathcal{O}(1/\Lambda_\chi m_N)$ . Section 5 contains the vector meson estimate of the chiral counterterms and the determination of the sign, while Section 6 gives our numerical estimate of the AM contributions to  $R_A^{T=0,1}$ . We briefly discuss the phenomenology of hadronic and nuclear PV and what that phenomenology may imply about the scale of the unknown low-energy constants. Section 7 summarizes our conclusions. The Appendices give a detailed discussion of (A) our formalism, (B) the full set of hadronic PV Lagrangians allowed under SU(3) symmetry, and (C) graphs, nominally present at  $\mathcal{O}(1/\Lambda_\chi^2)$  but whose contributions vanish.

## II. ANAPOLE CONTRIBUTIONS TO $R_A$

The electron-nucleon parity violating amplitude is generated by the diagrams in Figure 2. At tree level this amplitude reads

$$iM^{PV} = iM_{AV}^{PV} + iM_{VA}^{PV}, \quad (5)$$

where

$$iM_{AV}^{PV} = i \frac{G_\mu}{2\sqrt{2}} l^{\lambda 5} \langle N | J_\lambda | N \rangle \quad (6)$$

and

$$\begin{aligned} iM_{VA}^{PV} &= i \frac{G_\mu}{2\sqrt{2}} l^\lambda \langle N | J_{\lambda 5} | N \rangle \\ &= -i \frac{1 - 4\sin^2\theta_W}{2\sqrt{2}} g_A G_\mu \bar{e} \gamma^\lambda e \bar{N} \tau_3 \gamma_\lambda \gamma_5 N. \end{aligned} \quad (7)$$

at tree-level in the Standard Model (Figure 2a). Here,  $J_\lambda$  ( $J_{\lambda 5}$ ) and  $l_\lambda$  ( $l_{\lambda 5}$ ) denote the vector (axial vector) weak neutral currents of the quarks and electron, respectively [2].

The anapole moment interaction of Eq. (4) generates additional contributions to  $M_{VA}^{PV}$  when a photon is exchanged between the nucleon and the electron (Figure 2b). The corresponding amplitude is

$$iM_{AM}^{PV} = i \frac{(4\pi\alpha)}{\Lambda_\chi^2} \bar{e} \gamma^\lambda e \bar{N} (a_s + a_v \tau_3) \gamma_\lambda \gamma_5 N \quad . \quad (8)$$

Note that unlike  $iM_{VA}^{PV}$ ,  $iM_{AM}^{PV}$  contains no  $(1 - 4\sin^2 \theta_W)$  suppression. Consequently, the relative importance of the anapole interaction is enhanced by  $1/(1 - 4\sin^2 \theta_W) \sim 10$ . This enhancement may be seen explicitly by converting Eqs. (6) and (8) into  $R_A^{T=0,1}$ :

$$R_A^{T=0}|_{\text{anapole}} = -\frac{8\sqrt{2}\pi\alpha}{G_\mu \Lambda_\chi^2} \frac{1}{1 - 4\sin^2 \theta_W} \frac{a_s}{g_A} \quad (9)$$

$$R_A^{T=1}|_{\text{anapole}} = -\frac{8\sqrt{2}\pi\alpha}{G_\mu \Lambda_\chi^2} \frac{1}{1 - 4\sin^2 \theta_W} \frac{a_v}{g_A} \quad (10)$$

The constants  $a_{s,v}$  contain contributions from loops generated by the Lagrangians given in Section 3 and from counterterms in the tree-level effective Lagrangian of Eq. (4):

$$a_{s,v} = a_{s,v}^L + a_{s,v}^{CT} \quad . \quad (11)$$

In HBCPT, only the parts of the loop amplitudes non-analytic in quark masses can be unambiguously identified with  $a_{s,v}^L$ . The remaining analytic terms are included in  $a_{s,v}^{CT}$ . In what follows, we compute explicitly the various loop contributions up through  $\mathcal{O}(1/\Lambda_\chi^2)$ , while in principle,  $a_{s,v}^{CT}$  should be determined from experiment. In Section 5, however, we discuss a model estimate for  $a_{s,v}^{CT}$ .

Before proceeding with details of the calculation, it is useful to take note of the scales present in Eqs. (9). The constants  $a_{s,v}$  are generally proportional to a product of strong and weak meson-baryon couplings. The former are generally of order unity, while the size of weak, PV couplings can be expressed in terms of  $g_\pi = 3.8 \times 10^{-8}$ , the scale of charged current contributions [14]. One then expects the AM contributions to the axial radiative corrections to be of order

$$R_A^{T=0,1} \sim -\frac{8\sqrt{2}\pi\alpha}{G_\mu \Lambda_\chi^2} \frac{1}{1 - 4\sin^2 \theta_W} \frac{g_\pi}{g_A} \approx 0.01 \quad . \quad (12)$$

In some cases, the PV hadronic couplings may be an order of magnitude larger than  $g_\pi$ . Alternatively, chiral singularities arising from loops may also enhance the AM effects over the scale in Eq. (12). Thus, as we show below, the net effect of the AM is anticipated to be a 10-20 % contribution to  $R_A^{T=0,1}$ .

### III. NOTATIONS AND CONVENTIONS

Since much of the formalism for HBChPT is standard, we relegate a detailed summary of our conventions to Appendix A. However, some discussion of the effective Lagrangians used in computing chiral loop contributions to  $a_{s,v}$  is necessary here. Specifically, we require the parity-conserving (PC) and parity-violating (PV) Lagrangians involving pseudoscalar meson, spin-1/2 and spin-3/2 baryon, and photon fields. For the moment, we restrict ourselves to SU(2) flavor symmetry and generalize to SU(3) later. The relativistic PC Lagrangian for  $\pi$ ,  $N$ ,  $\Delta$ , and  $\gamma$  interactions needed here is

$$\begin{aligned} \mathcal{L}^{PC} = & \frac{F_\pi^2}{4} Tr D^\mu \Sigma D_\mu \Sigma^\dagger + \bar{N}(i\mathcal{D}_\mu \gamma^\mu - m_N)N + g_A \bar{N} A_\mu \gamma^\mu \gamma_5 N \\ & + \frac{e}{\Lambda_\chi} \bar{N}(c_s + c_v \tau_3) \sigma^{\mu\nu} F_{\mu\nu}^+ N \\ & - T_i^\mu [(i\mathcal{D}_\alpha^{ij} \gamma^\alpha - m_\Delta \delta^{ij}) g_{\mu\nu} - \frac{1}{4} \gamma_\mu \gamma^\lambda (i\mathcal{D}_\alpha^{ij} \gamma^\alpha - m_\Delta \delta^{ij}) \gamma_\lambda \gamma^\nu \\ & + \frac{g_1}{2} g_{\mu\nu} A_\alpha^{ij} \gamma^\alpha \gamma_5 + \frac{g_2}{2} (\gamma_\mu A_\nu^{ij} + A_\mu^{ij} \gamma_\nu) \gamma_5 + \frac{g_3}{2} \gamma_\mu A_\alpha^{ij} \gamma^\alpha \gamma_5 \gamma_\nu] T_j^\nu \\ & + g_{\pi N \Delta} [\bar{T}_i^\mu (g_{\mu\nu} + z_0 \gamma_\mu \gamma_\nu) \omega_i^\nu N + \bar{N} \omega_i^\nu (g_{\mu\nu} + z_0 \gamma_\nu \gamma_\mu) T_i^\mu] \\ & - ie \frac{c_\Delta q_i}{\Lambda_\chi} \bar{T}_i^\mu F_{\mu\nu}^+ T_i^\nu + [\frac{ie}{\Lambda_\chi} \bar{T}_3^\mu (d_s + d_v \tau_3) \gamma^\nu \gamma_5 F_{\mu\nu}^+ N + h.c.] \end{aligned} \quad (13)$$

where  $\mathcal{D}_\mu$  is a chiral and electromagnetic (EM) covariant derivative,  $\Sigma = \exp(i\vec{\tau} \cdot \vec{\pi}/F_\pi)$  is the conventional non-linear representation of the pseudoscalar field,  $N$  is a nucleon isodoublet field,  $T_\mu^i$  is the  $\Delta$  field in the isospurion formalism,  $F^{\mu\nu}$  is the photon field strength tensor, and  $A_\mu$  is the axial field involving the pseudoscalars

$$A_\mu = -\frac{D_\mu \pi}{F_\pi} + \mathcal{O}(\pi^3) \quad (14)$$

with  $D_\mu$  being the EM covariant derivative. Explicit expressions for the fields and the transformation properties can be found in Appendix A. The constants  $c_s, c_v$  determined in terms of the nucleon isoscalar and isovector magnetic moments,  $c_\Delta$  is the  $\Delta$  magnetic moment,  $d_s, d_v$  are the nucleon and delta transition magnetic moments, and  $z_0$  is the off-shell parameter which is not relevant in the present work [15]. Our convention for  $\gamma_5$  is that of Bjorken and Drell [16].

In order to obtain proper chiral counting for the nucleon, we employ the conventional heavy baryon expansion of  $\mathcal{L}^{PC}$ , and in order to consistently include the  $\Delta$  we follow the small scale expansion proposed in [15]. In this approach energy-momenta and the delta and nucleon mass difference  $\delta$  are both treated as  $\mathcal{O}(\epsilon)$  in chiral power counting. The leading order vertices in this framework can be obtained via  $P_+ \Gamma P_+$  where  $\Gamma$  is the original vertex in the relativistic Lagrangian and

$$P_\pm = \frac{1 \pm \not{v}}{2} \quad . \quad (15)$$

are projection operators for the large, small components of the Dirac wavefunction respectively. Likewise, the  $O(1/m_N)$  corrections are generally proportional to  $P_+\Gamma P_-/m_N$ . In previous work the parity conserving  $\pi N \Delta \gamma$  interaction Lagrangians have been obtained to  $O(1/m_N^2)$  [15]. We collect some of the relevant terms below:

$$\begin{aligned} \mathcal{L}_v^{PC} = & \bar{N}[iv \cdot D + 2g_A S \cdot A]N - i\bar{T}_i^\mu [iv \cdot D^{ij} - \delta^{ij}\delta + g_1 S \cdot A^{ij}]T_\mu^j \\ & + g_{\pi N \Delta} [\bar{T}_i^\mu \omega_\mu^i N + \bar{N} \omega_\mu^{i\dagger} T_i^\mu] \\ & + \frac{1}{2m_N} \bar{N} \{ (v \cdot D)^2 - D^2 + [S_\mu, S_\nu][D^\mu, D^\nu] \\ & - ig_A (S \cdot D v \cdot A + v \cdot A S \cdot D) \} N + \dots \end{aligned} \quad (16)$$

where  $S_\mu$  is the Pauli-Lubanski spin operator and  $\delta \equiv m_\Delta - m_N$ .

The PV analog of Eq. (13) can be constructed using the chiral fields  $X_{L,R}^a$  defined in Appendix A and the spacetime transformation properties of the various fields in Eq. (13). We find it convenient to follow the convention in Ref. [9] and separate the PV Lagrangian into its various isospin components. The hadronic weak interaction has the form

$$\mathcal{H}_w = \frac{G_\mu}{\sqrt{2}} J_\lambda J^\lambda{}^\dagger + \text{h.c.} , \quad (17)$$

where  $J_\lambda$  denotes either a charged or neutral weak current built out of quarks. In the Standard Model, the strangeness conserving charged currents are pure isovector, whereas the neutral currents contain both isovector and isoscalar components. Consequently,  $\mathcal{H}_w$  contains  $\Delta T = 0, 1, 2$  pieces and these channels must all be accounted for in any realistic hadronic effective theory.

Again for simplicity, we restrict our attention first to the light quark SU(2) sector. (A general SU(3) PV meson-baryon Lagrangian is given in the Appendix and is considerably more complex.) We quote the relativistic Lagrangians, but employ the heavy baryon projections, as described above, in computing loops. It is straightforward to obtain the corresponding heavy baryon Lagrangians from those listed below, so we do not list the PV heavy baryon terms below. For the  $\pi N$  sector we have

$$\mathcal{L}_{\Delta T=0}^{\pi N} = h_V^0 \bar{N} A_\mu \gamma^\mu N \quad (18)$$

$$\begin{aligned} \mathcal{L}_{\Delta T=1}^{\pi N} = & \frac{h_V^1}{2} \bar{N} \gamma^\mu N \text{Tr}(A_\mu X_+^3) - \frac{h_A^1}{2} \bar{N} \gamma^\mu \gamma_5 N \text{Tr}(A_\mu X_-^3) \\ & - \frac{h_\pi}{2\sqrt{2}} F_\pi \bar{N} X_-^3 N \end{aligned} \quad (19)$$

$$\begin{aligned} \mathcal{L}_{\Delta T=2}^{\pi N} = & h_V^2 \mathcal{I}^{ab} \bar{N} [X_R^a A_\mu X_R^b + X_L^a A_\mu X_L^b] \gamma^\mu N \\ & - \frac{h_A^2}{2} \mathcal{I}^{ab} \bar{N} [X_R^a A_\mu X_R^b - X_L^a A_\mu X_L^b] \gamma^\mu \gamma_5 N . \end{aligned} \quad (20)$$

The above Lagrangian was first given by Kaplan and Savage (KS) [9]. However, the coefficients used in our work are slightly different from those of Ref. [9] since our definition

of  $A_\mu$  differs by an overall phase (see Appendix A). Moreover, the coefficient of the second term in the original PV  $\Delta T = 2 NN\pi\pi$  Lagrangian in Eq. (2.18) was misprinted in the work of KS, and should be  $2h_A^2$  in their notation instead of  $h_V^2$  as given in Eq. (2.18) of [9].

The term proportional to  $h_\pi$  contains no derivatives and, at leading-order in  $1/F_\pi$ , yields the PV  $NN\pi$  Yukawa coupling traditionally used in meson-exchange models for the PV NN interaction [14,17]. The PV  $\gamma$ -decay of  $^{18}\text{F}$  can be used to constrain the value of  $h_\pi$  in a nuclear model-independent way as discussed in Ref. [17], resulting in  $h_\pi = (0.7 \pm 2.2)g_\pi$  [13]. Future PV experiments are planned using light nuclei to confirm the  $^{18}\text{F}$  result. The coupling  $h_\pi$  has also received considerable theoretical attention [14,27,18,19] and is particularly interesting since it receives no charged current contributions at leading order.

Unlike the PV Yukawa interaction, the vector and axial vector terms in Eqs. (18-20) contain derivative interactions. The terms containing  $h_A^1, h_A^2$  start off with  $NN\pi\pi$  interactions, while all the other terms start off as  $NN\pi$ . Such derivative interactions have not been included in conventional analyses of nuclear and hadronic PV experiments. Consequently, the experimental constraints on the low-energy constants  $h_V^i, h_A^i$  are unknown. The authors of Ref. [9] used simple dimensional arguments and factorization limits to estimate their values, and we present additional phenomenological considerations in Section 6 below. We emphasize, however, that the present lack of knowledge of these couplings introduces additional uncertainties into  $R_A^{T=0,1}$ .

In addition to purely hadronic PV interactions, one may also write down PV EM interactions involving baryons and mesons<sup>†</sup>. The anapole interaction of Eq. (4) represents one such interaction, arising at  $\mathcal{O}(1/\Lambda_\chi^2)$  and involving no  $\pi$ 's. There also exist terms at  $\mathcal{O}(1/\Lambda_\chi)$  which include at least one  $\pi$ :

$$\mathcal{L}^{\gamma N}_{PV} = \frac{c_1}{\Lambda_\chi} \bar{N} \sigma^{\mu\nu} [F_{\mu\nu}^+, X_-^3]_+ N + \frac{c_2}{\Lambda_\chi} \bar{N} \sigma^{\mu\nu} F_{\mu\nu}^- N + \frac{c_3}{\Lambda_\chi} \bar{N} \sigma^{\mu\nu} [F_{\mu\nu}^-, X_+^3]_+ N . \quad (21)$$

The corresponding PV Lagrangians involving a  $N \rightarrow \Delta$  transition are somewhat more complicated. The analogues of Eqs. (18-20) are

$$\begin{aligned} \mathcal{L}_{\Delta I=0}^{\pi \Delta N} = & f_1 \epsilon^{abc} \bar{N} i \gamma_5 [X_L^a A_\mu X_L^b + X_R^a A_\mu X_R^b] T_c^\mu \\ & + g_1 \bar{N} [A_\mu, X_-^a]_+ T_a^\mu + g_2 \bar{N} [A_\mu, X_-^a]_+ T_a^\mu + \text{h.c.} \end{aligned} \quad (22)$$

$$\begin{aligned} \mathcal{L}_{\Delta I=1}^{\pi \Delta N} = & f_2 \epsilon^{ab3} \bar{N} i \gamma_5 [A_\mu, X_+^a]_+ T_b^\mu + f_3 \epsilon^{ab3} \bar{N} i \gamma_5 [A_\mu, X_+^a]_- T_b^\mu \\ & + g_3 \bar{N} [(X_L^a A_\mu X_L^3 - X_L^3 A_\mu X_L^a) - (X_R^a A_\mu X_R^3 - X_R^3 A_\mu X_R^a)] T_a^\mu \\ & + g_4 \{ \bar{N} [3X_L^3 A^\mu (X_L^1 T_\mu^1 + X_L^2 T_\mu^2) + 3(X_L^1 A^\mu X_L^3 T_\mu^1 + X_L^2 A^\mu X_L^3 T_\mu^2) \\ & - 2(X_L^1 A^\mu X_L^1 + X_L^2 A^\mu X_L^2 - 2X_L^3 A^\mu X_L^3) T_\mu^3] - (L \leftrightarrow R) \} + \text{h.c.} \end{aligned} \quad (23)$$

---

<sup>†</sup>Note that the hadronic derivative interactions of Eqs. (18-20) also contain  $\gamma$  fields as required by gauge-invariance

$$\begin{aligned}\mathcal{L}_{\Delta I=2}^{\pi\Delta N} = & f_4 \epsilon^{abd} \mathcal{I}^{cd} \bar{N} i \gamma_5 [X_L^a A_\mu X_L^b + X_R^a A_\mu X_R^b] T_c^\mu \\ & + f_5 \epsilon^{ab3} \bar{N} i \gamma_5 [X_L^a A_\mu X_L^3 + X_L^3 A_\mu X_L^a + (L \leftrightarrow R)] T_b^\mu \\ & + g_5 \mathcal{I}^{ab} \bar{N} [A_\mu, X_-^a]_+ T_b^\mu + g_6 \mathcal{I}^{ab} \bar{N} [A_\mu, X_-^a]_+ T_b^\mu + \text{h.c.} \quad ,\end{aligned}\quad (24)$$

where the terms containing  $f_i$  and  $g_i$  start off with single and two pion vertices, respectively.

Finally, we consider PV  $\gamma\Delta N$  interactions:

$$\mathcal{L}_{PV}^{\gamma\Delta N} = ie \frac{d_1}{\Lambda_\chi} \bar{T}_3^\mu \gamma^\nu F_{\mu\nu}^+ N + ie \frac{d_2}{\Lambda_\chi} \bar{T}_3^\mu \gamma^\nu [F_{\mu\nu}^+, X_+]_+ N \quad (25)$$

$$\begin{aligned}& + ie \frac{d_3}{\Lambda_\chi} \bar{T}_3^\mu \gamma^\nu [F_{\mu\nu}^+, X_+]_- N + ie \frac{d_4}{\Lambda_\chi} \bar{T}_3^\mu \gamma^\nu \gamma_5 F_{\mu\nu}^- N \\ & + ie \frac{d_5}{\Lambda_\chi} \bar{T}_3^\mu \gamma^\nu \gamma_5 [F_{\mu\nu}^+, X_-^3]_+ N + ie \frac{d_6}{\Lambda_\chi} \bar{T}_3^\mu \gamma^\nu \gamma_5 [F_{\mu\nu}^-, X_+]_+ N \\ & + ie \frac{d_7}{\Lambda_\chi} \bar{T}_3^\mu \gamma^\nu [F_{\mu\nu}^-, X_-^3]_+ N + ie \frac{d_8}{\Lambda_\chi} \bar{T}_3^\mu \gamma^\nu [F_{\mu\nu}^-, X_-^3]_- N + \text{h.c.}\end{aligned}\quad (26)$$

The PV  $\gamma\Delta N$  vertices  $d_{1-3}$ ,  $d_{4-6}$  and  $d_{7-8}$  are associated at leading order in  $1/F_\pi$  with zero, one and two pion vertices, respectively. All the vertices in (18)-(25) are  $\mathcal{O}(p)$  or  $\mathcal{O}(1/\Lambda_\chi)$  except  $h_\pi$ , which is Yukawa interaction and of  $\mathcal{O}(p^0)$ . As we discuss in Appendix C, we do not require PV interactions involving two  $\Delta$  fields.

#### IV. CHIRAL LOOPS

The contributions to  $a_{s,v}$  arising from the Lagrangians of Eqs. (18-20) are shown in Figure 3. We regulate the associated integrals using dimensional regularization (DR) and absorb the divergent  $-1/(d-4)$  terms into the counterterms,  $a_{s,v}^{CT}$ . The leading contributions arise from the PV Yukawa coupling  $h_\pi$  contained in the loops of 3a-f. To  $\mathcal{O}(1/\Lambda_\chi^2)$ , the diagrams 3e,f containing a photon insertion on a nucleon line do not contribute. The reason is readily apparent from examination of the integral associated with the amplitude of Figure 3e:

$$\begin{aligned}iM_{3e} = & ie_N h_\pi v \cdot \varepsilon \frac{\sqrt{2}g_A}{F_\pi} \int \frac{d^D k}{(2\pi)^D} \frac{i(S \cdot k)}{v \cdot k} \frac{i}{v \cdot (q+k)} \frac{i}{k^2 - m_\pi^2 + i\epsilon} \\ = & -ie_N h_\pi v \cdot \varepsilon \frac{2\sqrt{2}g_A}{F_\pi} S_\mu \int_0^\infty s ds \int_0^1 du \int \frac{d^D k}{(2\pi)^D} \frac{k_\mu}{[k^2 + sv \cdot k + usv \cdot q + m_\pi^2]^3} ,\end{aligned}\quad (27)$$

where  $q_\mu$  is the photon momentum,  $\varepsilon$  is the photon polarization vector,  $s$  has the dimensions of mass, and we have Wick rotated to Euclidean momenta in the second line. From this form it is clear that  $iM_{3e} \propto S \cdot v = 0$ . The sum of the non-vanishing diagrams Figure 3a-d yields a gauge invariant leading order result, which is purely isoscalar:

$$a_s^L(Y1) = -\frac{\sqrt{2}}{24} e g_A h_\pi \frac{\Lambda_\chi}{m_\pi} . \quad (28)$$

As the PV Yukawa interaction is of order  $O(p^0)$ , we need to consider higher order corrections involving this interaction, which arise from the  $1/m_N$  expansion of the nucleon propagator and various vertices. Since  $P_+ \cdot 1 \cdot P_- = 0$ , there is no  $1/m_N$  correction to the PV Yukawa vertex. From the  $1/m_N \bar{N}N$  terms in Eq. (13) we have

$$a_s^L(Y2) = \frac{7\sqrt{2}}{48\pi} e g_A h_\pi \frac{\Lambda_\chi}{m_N} \ln\left(\frac{\mu}{m_\pi}\right)^2 , \quad (29)$$

where  $\mu$  is the subtraction scale introduced by DR. Finally, the  $1/m_N$  correction to the strong  $\pi NN$  vertex, contained in the term  $\propto g_A$  in Eq. (13), yields

$$a_s^L(Y3) = -\frac{\sqrt{2}}{48\pi} e g_A h_\pi \frac{\Lambda_\chi}{m_N} \ln\left(\frac{\mu}{m_\pi}\right)^2 . \quad (30)$$

These terms are also isoscalar, and the results in Eqs. (28-30) are fully contained in the previous analyses of Refs. [4,5,9].

For the interactions in Eqs. (18-20) containing  $h_V^i$ , the eight diagrams Figure 3a-h must be considered. Their contribution is purely isovector—

$$a_v^L(V) = \frac{1}{6} e g_A \left( h_V^0 + \frac{4}{3} h_V^2 \right) \ln\left(\frac{\mu}{m_\pi}\right)^2 . \quad (31)$$

—and was not included in previous analyses.

The contribution generated from the two-pion PV axial vertices in Eqs. (19-20) comes only from the loop Figure 3i and contains both isovector and isoscalar components:

$$a_s^L(A) + a_v^L(A)\tau_3 = -\frac{1}{3} e (h_A^1 + h_A^2 \tau_3) \ln\left(\frac{\mu}{m_\pi}\right)^2 . \quad (32)$$

a result first computed in Ref. [9].

In principle, a variety of additional contributions will arise at  $\mathcal{O}(1/\Lambda_\chi^2)$ . For example, insertion of the nucleon magnetic moments (*i.e.* the terms in Eq. (13) containing  $c_{s,v}$ ) into the loops Figure 3e,f—resulting in the loops of Figure 5a,b—would in principle generate terms of  $\mathcal{O}(1/\Lambda_\chi^2)$  when the PV Yukawa interaction is considered. As shown in Appendix C, however, such contributions vanish at this order. Similarly, the entire set of  $\Delta$  intermediate state contributions shown in Figure 4, as well as those generated by  $\mathcal{L}_{PV}^{\gamma N}$  and  $\mathcal{L}_{PV}^{\gamma \Delta N}$  in Figure 6, vanish up to  $\mathcal{O}(1/\Lambda_\chi^2)$ . The reasons for the vanishing of these various possible contributions is discussed in Appendix C. Thus, the complete set of SU(2) loop contributions up to  $\mathcal{O}(1/\Lambda_\chi^2)$  are given in Eqs. (28-32).

Because  $m_c - m_s \gg m_s - m_{u,d}$  and  $\Lambda_\chi \gg m_s$ , it may be appropriate to treat the lightest strange and non-strange hadrons on a similar footing and extend the foregoing discussion to SU(3) chiral symmetry. A similar philosophy has been adopted by several authors in studying the axial charges and magnetic moments of the lightest baryons

[10,20–23]. In what follows, we consider the possibility that kaon loop contributions, introduced by the consideration of SU(3) symmetry, may further enhance the anapole contribution to  $R_A$ .

Before proceeding along these lines, however, one must raise an important caveat. When kaon loop corrections are included in a HBChPT analysis, higher order chiral corrections may go as powers of  $m_K/\Lambda_\chi \sim 0.5$ . Consequently, the convergence of the SU(3) chiral expansion remains a subject of debate [24]. Fortunately, no such factors appear in the present analysis through  $\mathcal{O}(1/\Lambda_\chi^2)$  so that at this order, we find that kaon loop effects in  $R_A$  are generally tiny compared to those involving pion loops. Whether or not higher-order terms (*e.g.*, those of  $\mathcal{O}(1/\Lambda_\chi^2 \times m_K/\Lambda_\chi)$ ) contribute as strongly as those considered here remains a separate, open question.

To set our notation, we give the leading strong-interaction SU(3) Lagrangian. Since the  $K^0$  and  $\eta$  are neutral, loops containing these mesons do not contribute to the AM through  $\mathcal{O}(1/\Lambda_\chi^2)$  and we do not include their strong couplings below. For the proton the possible intermediate states are  $\Sigma^0 K^+$ ,  $\Lambda K^+$  while for the neutron only  $\Sigma^- K^+$  can appear. The necessary vertices derive from

$$\begin{aligned} \mathcal{L} = & 2g_A \bar{N} S \cdot AN + 2g_{N\Lambda K}[(\bar{N} S \cdot K)\Lambda + \bar{\Lambda}(S \cdot K^\dagger N)] \\ & + 2g_{N\Sigma K}[S \cdot K^\dagger \bar{\Sigma} N + \bar{N} \Sigma S \cdot K], \end{aligned} \quad (33)$$

where  $g_{N\Lambda K} = -[(1 + 2\alpha)/\sqrt{6}]g_A$ ,  $g_{N\Sigma K} = (1 - 2\alpha)g_A$  with  $g_A = D + F$ ,  $\alpha = F/(D + F)$  and  $D, F$  are the usual  $SU(3)$  symmetric and antisymmetric coupling constants.

The general pseudoscalar octet and baryon octet PV Lagrangians are given in the Appendix B. They contain four independent PV Yukawa couplings, 20 axial vector couplings ( $h_A$ -type), and 22 vector couplings ( $h_V$ -type). For simplicity, we combine the  $SU(3)$  couplings into combinations specific to various hadrons—*e.g.* the leading PV Yukawa interactions are

$$\begin{aligned} \mathcal{L}_{\text{Yukawa}}^{1\pi} = & -ih_\pi(\bar{p}n\pi^+ - \bar{n}p\pi^-) - ih_{p\Sigma^0 K}(\bar{p}\Sigma^0 K^+ - \bar{\Sigma}^0 pK^-) \\ & - ih_{n\Sigma^- K}(\bar{n}\Sigma^- K^+ - \bar{\Sigma}^- nK^-) - ih_{p\Lambda K}(\bar{p}\Lambda K^+ - \bar{\Lambda}pK^-) + \dots \end{aligned} \quad (34)$$

In terms of the  $SU(3)$  couplings listed in Appendix B, the  $h_{BBM}$  have the form

$$\begin{aligned} h_\pi &= -2\sqrt{2}(h_1 + h_2) \\ h_{p\Sigma^0 K} &= -[h_1 - h_2 + \sqrt{3}(h_3 - h_4)] \\ h_{n\Sigma^- K} &= \sqrt{2}h_{p\Sigma^0 K} \\ h_{p\Lambda K} &= \left[ \frac{h_1}{\sqrt{3}} + \sqrt{3}h_2 + h_3 + 3h_4 \right] \quad . \end{aligned} \quad (35)$$

Similarly, we write for the vector PV interaction

$$\begin{aligned} \mathcal{L}_V^{1\pi} = & -\frac{h_V^{pn\pi^+}}{\sqrt{2}F_\pi}\bar{p}\gamma^\mu n D_\mu \pi^+ - \frac{h_V^{p\Sigma^0 K^+}}{\sqrt{2}F_\pi}\bar{p}\gamma^\mu \Sigma^0 D_\mu K^+ \\ & -\frac{h_V^{n\Sigma^- K^+}}{\sqrt{2}F_\pi}\bar{n}\gamma^\mu \Sigma^- D_\mu K^+ - \frac{h_V^{p\Lambda K^+}}{\sqrt{2}F_\pi}\bar{p}\gamma^\mu \Lambda D_\mu K^+ + h.c. + \dots , \end{aligned} \quad (36)$$

and for the axial PV two pion and kaon interactions

$$\begin{aligned}
\mathcal{L}_A^{2\pi} = & i \frac{h_A^{p\pi}}{F_\pi^2} \bar{p} \gamma^\mu \gamma_5 p (\pi^+ D_\mu \pi^- - \pi^- D_\mu \pi^+) + i \frac{h_A^{pK}}{F_\pi^2} \bar{p} \gamma^\mu \gamma_5 p (K^+ D_\mu K^- - K^- D_\mu K^+) \\
& + i \frac{h_A^{n\pi}}{F_\pi^2} \bar{n} \gamma^\mu \gamma_5 n (\pi^+ D_\mu \pi^- - \pi^- D_\mu \pi^+) + i \frac{h_A^{nK}}{F_\pi^2} \bar{n} \gamma^\mu \gamma_5 n (K^+ D_\mu K^- - K^- D_\mu K^+) \\
& + \dots
\end{aligned} \tag{37}$$

Expressions for these PV vector and axial coupling constants in terms of SU(3) constants appear in Appendix B. For illustrative purposes, it is useful to express the nucleon-pion couplings in terms of the  $h_{V,A}^i$  of Eqs. (18-20) for the SU(2) sector:

$$\begin{aligned}
h_V^{pn\pi^+} &= h_V^0 + \frac{4}{3} h_V^2 \\
h_A^{p\pi} &= h_A^1 + h_A^2 \\
h_A^{n\pi} &= h_A^1 - h_A^2
\end{aligned} \tag{38}$$

The leading order contributions to  $a_{s,v}$  arise only from the loops in Figure 3 where a photon couples to a charged meson. The charged kaon loop contributions to the  $a_{s,v}$  can be obtained from the corresponding formulae for the  $\pi$ -loop terms by making simple replacements of couplings and masses. For example, for the PV Yukawa interactions, these replacements are: (a) for the proton case,  $m_\pi \rightarrow m_K$ ,  $h_\pi \rightarrow h_{p\Sigma^0 K}$ ,  $g_A \rightarrow g_{N\Sigma^0 K^+} = g_{N\Sigma K}/\sqrt{2}$  for  $\Sigma^0 K^+$  intermediate states and  $h_\pi \rightarrow h_{p\Lambda K}$ ,  $g_A \rightarrow g_{N\Lambda K}$  for  $\Lambda K^+$ ; (b) for the neutron case,  $h_\pi \rightarrow h_{n\Sigma^- K}$ ,  $g_A \rightarrow g_{N\Sigma^- K^+} = g_{N\Sigma K}$  for  $\Sigma^- K^+$  intermediate state for the neutron case. Similar replacements hold for the vector PV coupling contributions. For the axial PV two-pion contribution we need only make the replacement  $h_A^{p\pi} \rightarrow h_A^{pK}$ ,  $m_\pi \rightarrow m_K$ .

Upon making these substitutions, we obtain the complete heavy baryon loop contribution to  $\mathcal{O}(1/\Lambda_\chi^2)$  in SU(3):

$$\begin{aligned}
a_s^L &= \frac{\sqrt{2}}{24} g_A h_\pi \left[ -\frac{\Lambda_\chi}{m_\pi} + \frac{3}{\pi} \frac{\Lambda_\chi}{m_N} \ln\left(\frac{\mu}{m_\pi}\right)^2 \right] \\
&\quad - \frac{\sqrt{3}}{144} (1+2\alpha) g_A h_{p\Lambda K} \left[ -\frac{\Lambda_\chi}{m_K} + \frac{3}{\pi} \frac{\Lambda_\chi}{m_N} \ln\left(\frac{\mu}{m_K}\right)^2 \right] \\
&\quad + \frac{\sqrt{2}}{32} (1-2\alpha) g_A h_{n\Sigma^- K} \left[ -\frac{\Lambda_\chi}{m_K} + \frac{3}{\pi} \frac{\Lambda_\chi}{m_N} \ln\left(\frac{\mu}{m_K}\right)^2 \right] \\
&\quad - \frac{1}{6} (h_A^{p\pi} + h_A^{n\pi}) \ln\left(\frac{\mu}{m_\pi}\right)^2 - \frac{1}{6} (h_A^{pK} + h_A^{nK}) \ln\left(\frac{\mu}{m_K}\right)^2 \\
&\quad + \frac{1}{12} (1-2\alpha) g_A (h_V^{n\Sigma^- K^+} + \frac{h_V^{p\Sigma^0 K^+}}{\sqrt{2}}) \ln\left(\frac{\mu}{m_K}\right)^2 \\
&\quad - \frac{\sqrt{6}}{72} (1+2\alpha) g_A h_V^{p\Lambda K^+} \ln\left(\frac{\mu}{m_K}\right)^2 \\
a_v^L &= -\frac{\sqrt{2}}{96} (1-2\alpha) g_A h_{n\Sigma^- K} \left[ -\frac{\Lambda_\chi}{m_K} + \frac{3}{\pi} \frac{\Lambda_\chi}{m_N} \ln\left(\frac{\mu}{m_K}\right)^2 \right]
\end{aligned} \tag{39}$$

$$\begin{aligned}
& -\frac{\sqrt{3}}{144}(1+2\alpha)g_Ah_{p\Lambda K}[-\frac{\Lambda_\chi}{m_K}+\frac{3}{\pi}\frac{\Lambda_\chi}{m_N}\ln(\frac{\mu}{m_K})^2] \\
& -\frac{1}{6}(h_A^{p\pi}-h_A^{n\pi})\ln(\frac{\mu}{m_\pi})^2-\frac{1}{6}(h_A^{pK}-h_A^{nK})\ln(\frac{\mu}{m_K})^2 \\
& -\frac{1}{6}g_Ah_V^{pn\pi^+}\ln(\frac{\mu}{m_\pi})^2 \\
& +\frac{1}{12}(1-2\alpha)g_A(-h_V^{n\Sigma^-K^+}+\frac{h_V^{p\Sigma^0K^+}}{\sqrt{2}})\ln(\frac{\mu}{m_K})^2 \\
& -\frac{\sqrt{6}}{72}(1+2\alpha)g_Ah_V^{p\Lambda K^+}\ln(\frac{\mu}{m_K})^2. \tag{40}
\end{aligned}$$

## V. LOW-ENERGY CONSTANTS AND VECTOR MESONS

A pure ChPT treatment of the anapole contributions to  $R_A$  would use a measurement of the axial term in  $A_{LR}(ep)$  and  $A_{LR}(QE)$ , together with the non-analytic, long-distance loop contributions,  $a_{s,v}^L$ , to determine the low-energy constants,  $a_{s,v}^{CT}$ . In the present case, however, we wish to determine whether there exist reasonable hadronic mechanisms which can enhance the low-energy constants to the level suggested by the SAMPLE results. Thus, we attempt to estimate  $a_{s,v}^{CT}$  theoretically.

Because they are governed in part by the short-distance ( $r > 1/\Lambda_\chi$ ) strong interaction,  $a_{s,v}^{CT}$  are difficult to compute from first principles in QCD. Nevertheless, experience with ChPT in the pseudoscalar meson sector and with the phenomenology of nucleon EM form factors suggests a reasonable model approach. It is well known, for example, that in the  $\mathcal{O}(p^4)$  chiral Lagrangian describing pseudoscalar interactions, the low-energy constants are well-described by the exchange of heavy mesons [25]. In particular, the charge radius of the pion receives roughly a 7% long-distance loop contribution, while the remaining 93% is saturated by  $t$ -channel exchange of the  $\rho^0$ . Similarly, in the baryon sector, dispersion relation analyses of the isovector and isoscalar nucleon electromagnetic form factors indicate important contributions from the lightest vector mesons [26]. Thus, it seems reasonable to assume that  $t$ -channel exchange of vector mesons also plays an important role in the short-distance physics associated with the anapole moment.

With these observations in mind, we estimate the coefficients  $a_{s,v}^{CT}$  in the approximation that they are saturated by  $t$ -channel exchange of the lightest vector mesons, as shown in Figure 7. Here parity-violation enters through the vector meson-nucleon interaction vertices. We also use a similar picture for the electromagnetic nucleon form factors to determine the overall phase of  $a_{s,v}^{CT}$  in the vector meson dominance approximation. To that end we require the PC and PV vector meson-nucleon Lagrangians [14]:

$$\mathcal{L}_{\rho NN}^{PC} = g_{\rho NN}\bar{N}[\gamma_\mu + \kappa_\rho \frac{i\sigma_{\mu\nu}q^\nu}{2m_N}]\tau \cdot \rho^\mu N \tag{41}$$

$$\mathcal{L}_{\omega NN}^{PC} = g_{\omega NN}\bar{N}[\gamma_\mu + \kappa_\omega \frac{i\sigma_{\mu\nu}q^\nu}{2m_N}]\omega^\mu N \tag{42}$$

$$\mathcal{L}_{\phi NN}^{PC} = g_{\phi NN} \bar{N} [\gamma_\mu + \kappa_\phi \frac{i\sigma_{\mu\nu}q^\nu}{2m_N}] \phi^\mu N \quad (43)$$

and

$$\mathcal{L}_{\rho NN}^{PV} = \bar{N} \gamma^\mu \gamma_5 \rho_\mu^0 [h_\rho^1 + (h_\rho^0 + \frac{h_\rho^2}{\sqrt{6}}) \tau_3] N \quad (44)$$

$$\mathcal{L}_{\omega NN}^{PV} = \bar{N} \gamma^\mu \gamma_5 \omega_\mu [h_\omega^0 + h_\omega^1 \tau_3] N \quad (45)$$

$$\mathcal{L}_{\phi NN}^{PV} = \bar{N} \gamma^\mu \gamma_5 \phi_\mu [h_\phi^0 + h_\phi^1 \tau_3] N . \quad (46)$$

(Note that we have adopted a different convention for  $\gamma_5$  than used in Ref. [14].) The coupling constants  $h_{\rho, \omega, \phi}^i$  were estimated in Refs. [14,27] and have also been constrained by a variety of hadronic and nuclear parity-violating experiments (for a review, see Ref. [17]).

For the  $V - \gamma$  transition amplitude, we use

$$\mathcal{L}_{V\gamma} = \frac{e}{2f_V} F^{\mu\nu} V_{\mu\nu} , \quad (47)$$

where  $e$  is the charge unit,  $f_V$  is the  $\gamma$ - $V$  conversion constant ( $V = \rho^0, \omega, \phi$ ), and  $V_{\mu\nu}$  is the corresponding vector meson field tensor. (This gauge-invariant Lagrangian ensures that the diagrams of Figure 7 do not contribute to the charge of the nucleon.) The amplitude of Figure 7 then becomes

$$a_s^{CT}(VMD) = \frac{h_\rho^1}{f_\rho} \left( \frac{\Lambda_\chi}{m_\rho} \right)^2 + \frac{h_\omega^0}{f_\omega} \left( \frac{\Lambda_\chi}{m_\omega} \right)^2 + \frac{h_\phi^0}{f_\phi} \left( \frac{\Lambda_\chi}{m_\phi} \right)^2 , \quad (48)$$

$$a_v^{CT}(VMD) = \frac{h_\rho^0 + h_\rho^2/\sqrt{6}}{f_\rho} \left( \frac{\Lambda_\chi}{m_\rho} \right)^2 + \frac{h_\omega^1}{f_\omega} \left( \frac{\Lambda_\chi}{m_\omega} \right)^2 + \frac{h_\phi^1}{f_\phi} \left( \frac{\Lambda_\chi}{m_\phi} \right)^2 . \quad (49)$$

The parity violating rho-pole contribution was first derived in [4,5]. However, the relative sign between  $h_{\rho N}^i$  and  $f_\rho$  is undetermined from the diagram of Figure 7 alone. Nevertheless, we can fix the overall phase using two phenomenological inputs. Parity violating experiments in the p-p system constrain the sign of the combination  $g_{\rho N} h_{\rho N}^i$  [28,29,17]. In particular, the scale of the longitudinal analyzing power,  $A_L$ , is set by the combination of constants

$$A_L \propto g_{\rho NN} (2 + \kappa_V) [h_\rho^0 + h_\rho^1 + h_\rho^2/\sqrt{6}] + g_{\omega NN} (2 + \kappa_S) [h_\omega^0 + h_\omega^1] , \quad (50)$$

where the constant of proportionality is positive,  $\kappa_V = 3.7$  and  $\kappa_S = -0.12$ . Using the standard values for the strong  $VNN$  couplings, one finds that  $A_L$  has roughly the same sensitivity to each of the  $h_V^i$  appearing in Eq. (50) (modulo the  $1/\sqrt{6}$  coefficient of  $h_\rho^2$ ). From the 45 MeV experiment performed at SIN [30], for example, one obtains the approximate constraint [13]

$$h_\rho^0 + h_\rho^1 + h_\rho^2/\sqrt{6} + h_\omega^0 + h_\omega^1 \sim -28 \pm 4 , \quad (51)$$

where the  $h_V^i$  have are expressed in units of  $g_\pi$  and where a positive sign has been assumed for  $g_{VNN}$ . Given this constraint, it is very unlikely that the product  $(h_\rho^0 + h_\rho^2/\sqrt{6})g_{\rho NN} > 0$  unless the corresponding products involving  $h_\rho^1$  and  $h_\omega^{0,1}$  in Eq. (50) obtain anomalously large, negative values. In fact, a fit to hadronic and nuclear PV observables in Ref. [17] strongly favors a phase difference between the strong and weak  $VNN$  couplings.

Experimentally, one also knows the isovector nucleon charge radius

$$\langle r^2 \rangle_{EXP}^{T=1} = 6 \frac{dF_1(q^2)}{dq^2} \Big|_{q^2=0} > 0 , \quad (52)$$

where

$$\langle p' | j_\mu^{T=1}(0) | p \rangle = e \bar{u}(p') [F_1(q^2) + \frac{i\sigma_{\mu\nu}q^\nu}{2m_N} F_2(q^2)] u(p) . \quad (53)$$

One may reasonably approximate the  $\rho^0$  contribution to  $\langle r^2 \rangle^{T=1}$  using VMD [26]. The calculation is the same as above but with the weak hadronic coupling replaced by the strong coupling. The result is

$$F_1^{\rho^0}(q^2) = \frac{g_{\rho NN}}{f_\rho} \frac{q^2}{q^2 - m_\rho^2} . \quad (54)$$

Then we have

$$\frac{dF_1^{VMD}(q^2)}{dq^2} \Big|_{q^2=0} = -\frac{g_{\rho NN}}{f_\rho m_\rho^2} . \quad (55)$$

Comparing Eqs. (52) and (55), and noting that the  $\rho^0$  generates a positive contribution to  $\langle r^2 \rangle^{T=1}$  [26], we arrive at  $g_{\rho NN}/f_\rho < 0$ . Combining this result with  $g_{\rho NN}h_\rho^i < 0$  as favored by the  $\bar{p}p$  experiments [28,29,17] we obtain the relative sign between  $h_\rho^i$  and  $f_\rho$ :  $h_\rho^i/f_\rho > 0$ . Accordingly we determine the relative signs for PV  $\omega, \phi$ -nucleon coupling constants.

## VI. THE SCALE OF $R_A$

Expressions for the anapole contributions to  $R_A^{T=0}$  and  $R_A^{T=1}$  in terms of the  $a_{s,v}$  appear in Eq. (9). We may now use these expressions, along with the results in Eqs. (39-40) and (48-49), to obtain a numerical estimate for the  $R_A^{T=0,1}|_{\text{anapole}}$ . To do so, we use the global fit value for the weak mixing angle in the on-shell scheme,  $\sin^2 \theta_W = 0.2230$  [3],  $g_A = 1.267 \pm 0.004$  [3],  $f_\rho = 5.26$  [31],  $f_\omega = 17$ ,  $f_\phi = 13$  [32],  $\alpha = F/(D+F) = 0.36$ ,  $\mu = \Lambda_\chi$ . We express all the PV coupling constants in units of  $g_\pi = 3.8 \times 10^{-8}$  as is traditionally done [27,14]. We obtain

$$\begin{aligned}
R_A^{T=0}|_{\text{anapole}} = & 10^{-2} \{ 0.17h_\pi + h_A^1 - 0.0036h_{n\Sigma-K} \\
& - 0.033(h_V^{n\Sigma-K^+} + \frac{h_V^{p\Sigma^0K^+}}{\sqrt{2}}) + 0.2(h_A^{pK} + h_A^{nK}) - 0.006h_{p\Lambda K} \\
& + 0.088h_V^{p\Lambda K^+} - 0.26|h_\rho^1| - 0.08|h_\omega^0| - 0.05|h_\phi^0| \} \quad (56)
\end{aligned}$$

$$\begin{aligned}
R_A^{T=1}|_{\text{anapole}} = & 10^{-2} \{ h_A^2 - 0.6(h_V^0 + \frac{4}{3}h_V^2) - 0.0012h_{n\Sigma-K} - 0.033(-h_V^{n\Sigma-K^+} \\
& + \frac{h_V^{p\Sigma^0K^+}}{\sqrt{2}}) + 0.2(h_A^{pK} - h_A^{nK}) - 0.006h_{p\Lambda K} + 0.088h_V^{p\Lambda K^+} \\
& - 0.26(|h_\rho^0| + \frac{|h_\rho^2|}{\sqrt{6}}) - 0.087|h_\omega^1| + 0.05|h_\phi^1| \} , \quad (57)
\end{aligned}$$

where we have set the phase of the vector meson contributions as discussed above, and used the relations in Eq. (38).

The expressions in Eqs. (56-57) illustrate the sensitivity of the radiative corrections to the various PV hadronic couplings. As expected on general grounds, the overall scale of  $R_A^{T=0,1}$  is at about the one percent level [see Eq. (12)]. In terms of the conventional PV couplings,  $R_A^{T=0}$  is most sensitive to  $h_\pi$  and  $h_\rho^1$ , while  $R_A^{T=1}$  is most strongly influenced by  $h_\rho^0 + h_\rho^2/\sqrt{6}$ . The corrections also display strong dependences on the couplings  $h_{V,A}^i$  not included in the standard analysis of nuclear and hadronic PV. In particular, the couplings  $h_A^2$  and  $h_V^0 + 4h_V^2/3$  are weighted heavily in  $R_A^{T=1}$ . In general, the sensitivity to the PV  $NYK$  couplings is considerably weaker than the sensitivity to the  $NN\pi$  and  $NN\rho$  couplings.

In order to make an estimate of  $R_A^{T=0,1}$ , we require inputs for the PV couplings. To that end, we use the “best values” for  $h_\pi$ ,  $h_\rho^i$ , and  $h_\omega^i$  given in Ref. [27]. These values are consistent with the fit of Ref. [17]. For the  $h_\phi^i$  we use the “best values” of Ref. [14]. The analyses given in Refs. [14,17,27], together with experimental input, also allow for the standard couplings to take on a range of values. For example, the ranges for the  $h_\omega^i$  given in Refs. [14,27] correspond to

$$-33 \leq h_\omega^0 + h_\omega^1 \leq 13 \quad . \quad (58)$$

In order to maintain consistency with the experimental constraint of Eq. (51), one then requires

$$0 \leq h_\rho^0 + h_\rho^1 + h_\rho^2/\sqrt{6} \leq -45 \quad . \quad (59)$$

We adopt this range even though it is smaller than the range given in Ref. [27]. Indeed, allowing the  $h_\rho^i$  to assume the full ranges given in Ref. [27] would require the  $h_\omega^i$  to vary outside their corresponding theoretical “reasonable ranges” if the constraint of Eq. (51) is to be satisfied. Since one expects  $|h_\rho^1| \ll |h_\rho^{0,2}|$  [14,27], we have a reasonable range of values for the important isoscalar  $\rho$  contribution in Eq. (57), and the rather broad range of values allowed for the  $h_\rho^i$  contributes significantly to our estimated uncertainty

in  $R_A^{T=1}$ . For  $h_{\omega,\phi}^i$ , we use the ranges of Refs. [14,27]<sup>‡</sup>. In contrast to the situation with the  $h_\rho^0$  contribution, however, the variation in the  $h_{\omega,\phi}^i$  over their “reasonable ranges” has negligible impact on our estimated theoretical uncertainty.

Estimating values for the Yukawa couplings  $h_{NYK}$  and for the  $h_{V,A}$  is more problematic—to date, no calculation on the level of Ref. [14] has been performed for such couplings. Estimates for  $h_{V,A}$ , based on dimensional and factorization arguments, were given in Ref. [9] and generally yielded values for  $h_{V,A}$  in the non-strange sector on the order of  $g_\pi$ . For our central values, then, we take  $h_{V,A}^i = g_\pi$ , resulting in roughly 1% contributions from the PV vector and axial vector interactions. Without performing a detailed calculation as in Ref. [14], one might also attempt to determine reasonable ranges for these parameters by looking to phenomenology. To that end, the authors of Ref. [9] considered analogies between the axial vector PV operators of Eq. (19-20) and contact operators needed to explain the size of  $\Delta I = 1/2$  hyperon P-wave decay amplitudes. From this analogy, these authors conclude that  $|h_A^i| \sim 10g_\pi$  may be reasonable. However, whether such large ranges are consistent with nuclear PV data remains to be determined. In the absence of such an analysis, which goes beyond the scope of the present work, we adopt the range  $-10g_\pi \leq h_A^i \leq 10g_\pi$  suggested in Ref. [9]. The corresponding uncertainties in the  $R_A^{T=0,1}$  are roughly  $\pm 10\%$ .

The implications of phenomenology for the  $h_V^i$  are even less clear than for the  $h_A^i$ . However, we note that large values  $h_V^i \sim \pm 10g_\pi$  do not appear to be ruled out by hadronic and nuclear PV data. At tree-level, for example, the vector terms in  $\mathcal{L}_{\Delta T=0,1,2}^{\pi N}$  do not contribute to the PV NN interaction through the one  $\pi$ -exchange amplitudes of Figure 8a. It is straightforward to show that the corresponding amplitude vanishes for on-shell nucleons <sup>§</sup>. Thus, at this level, purely hadronic PV processes are insensitive to the  $h_V^i$  and provide no constraints on these couplings. In PV electromagnetic processes, however, the  $h_V^i$  do contribute through PV two-body currents, such as those shown in Figure 8b. Nevertheless, one expects the impact of PV two-body currents to be considerably weaker than that of the PV NN potential. The PV  $\gamma$ -decay of  $^{18}\text{F}$ , for example, is dominated by the mixing of a nearly-degenerate pair of  $(J^\pi, T) = (0^-, 0)$  and  $(0^+, 1)$  states. The small energy denominator associated with this parity-mixing enhances the relative importance of the PV NN potential by roughly two orders of magnitude over the generic situation with typical nuclear level spacings. By contrast, the PV two-body currents do not participate in parity-mixing and receive no such enhancements. A similar situation holds for PV electromagnetic processes in other nuclei of interest. Hence, we expect the PV  $\gamma$ -decays of light nuclei to be relatively insensitive to the  $h_V^i$ , even if the latter are on the order of  $10g_\pi$ . Consequently, we rather generously take  $-10g_\pi \leq h_V^0 + 4h_V^2/3 \leq 10g_\pi$ , yielding a

<sup>‡</sup>Allowing the  $h_\omega^i$  to assume positive values would require a sign change on the corresponding terms in Eqs. (56,57).

<sup>§</sup>The on-shell approximation is generally used in deriving the PV NN potential from Feynman diagrams.

$\pm 7\%$  contribution to the uncertainty in  $R_A^{T=1}$ . Allowing similarly large ranges for the PV  $NYK$  couplings has a negligible impact on the uncertainty in the  $R_A^{T=0,1}$ .

With these input values for the PV couplings, we arrive at the anapole contributions to  $R_A^{T=0,1}$  shown in Table I. The latter must be added to the one-quark Standard Model contributions, also shown in Table I. We compute the one-quark corrections using the on-shell parameters given in Ref. [3]. We emphasize that the quoted values for the  $R_A^{T=0,1}$  are renormalization scheme-dependent. The relative size of one-quark corrections are smaller, for example, in the  $\overline{MS}$  scheme. The corresponding tree-level amplitude, however, is also smaller than the on-shell tree-level amplitude. A reader working in the  $\overline{MS}$  scheme should, therefore, take care to adjust the tree-level amplitude and SM radiative corrections appropriately from the on-shell values used here.

Adding the one-quark and anapole contributions yields a large, negative value for  $R_A^{T=1}$ . This result contains considerable theoretical uncertainty, mostly due to our liberal assignment of reasonable ranges to the  $h_{V,A}$ . Even with this generous theoretical uncertainty, however,  $R_A^{T=1}$  is still roughly a factor of two away from the apparent SAMPLE result. Compared with the one-quark SM contribution, the many-quark anapole contribution is relatively small – though it does push the total in the right direction. The isoscalar correction,  $R_A^{T=0}$ , is considerably smaller in magnitude than  $R_A^{T=1}$  yet retains a sizeable theoretical uncertainty.

## TABLES

Source	$R_A^{T=1}$	$R_A^{T=0}$
One-quark (SM)	−0.35	−0.06
Anapole	$−0.06 \pm 0.24$	$0.01 \pm 0.14$
Total	$−0.41 \pm 0.24$	$−0.05 \pm 0.14$

TABLE I. One-quark Standard Model (SM) and many-quark anapole contributions to  $V(A) \times A(N)$  radiative corrections. Values are computed in the on-shell scheme using  $\sin^2 \theta_W = 0.2230$  .

## VII. CONCLUSIONS

In view of the preliminary SAMPLE result for PV quasielastic electron scattering from  $^2\text{H}$ , we have up-dated our previous calculation of the axial vector radiative corrections  $R_A^{T=0,1}$ . Using the framework of HBChPT, we have computed all many-quark anapole contributions through  $\mathcal{O}(1/\Lambda_\chi^2)$ . We include new one-loop contributions involving the PV vector couplings,  $h_V^i$  and estimate the scale of the analytic, low-energy constants using resonance saturation. We fix the sign of the latter using the phenomenology of PV  $\vec{p}\vec{p}$  scattering and of nucleon EM form factors. We also show that large classes of loops involving decuplet intermediate states, magnetic insertions, and PV EM insertions vanish through  $\mathcal{O}(1/\Lambda_\chi^2)$ . Finally, we extend the previous analyses to include SU(3) symmetry, and determine that the impact of kaon loops is generally negligible. In the end, we find that  $R_A^{T=1}$ —though large and negative—is still a factor of two or so away from the suggestion that  $R_A^{T=1} \sim -1$  from the SAMPLE experiment. Even allowing for considerable theoretical uncertainty – dominated by the PV couplings  $h_{V,A}^i$  – there remains a sizable gap between our result and the preliminary experimental value.

There exist a number of possible additional contributions to  $R_A^{T=0,1}$  not considered here which may ultimately account for the apparent experimental result. The most obvious include higher-order chiral corrections. This appears, however, to be an unlikely source of large contributions. On general grounds, we expect the size of the  $\mathcal{O}(1/\Lambda_\chi^3)$  contributions to be suppressed by  $m/\Lambda_\chi$  relative to those considered here, where  $m$  denotes a pseudoscalar mass. For kaon loops, this suppression factor is only  $\sim 1/2$ ; however, at  $\mathcal{O}(1/\Lambda_\chi^2)$  kaon loops generate at most a few percent contribution to  $R_A^{T=0,1}$ . The suppression factor for the next order pionic contributions is closer to 0.1. Hence, it would be surprising if the next order in the chiral expansion could close the factor of two gap with experiment.

More promising sources of sizeable contributions include  $Z - \gamma$  box graph contributions, where the full tower of hadronic intermediate states is included, as well as parity-mixing in the deuteron wavefunction. At a more speculative level, one might also consider contributions from physics beyond the Standard Model. For example, the presence of an additional, relatively light neutral gauge boson might modify the SM  $V(e) \times A(q)$  amplitudes and contribute to  $R_A^{T=1}$ . A popular class of  $Z'$  models are generated by  $E_6$  symmetry [33]. The contribution of an extra, neutral weak  $E_6$  gauge boson  $Z'$  is given by

$$R_A^{T=1}(\text{new}) = \frac{4}{5} \frac{1}{1 - 4\sin^2 \theta_W} \sin^2 \phi \frac{G'_\phi}{G_\mu} \quad , \quad (60)$$

where  $\phi$  is a mixing angle which governs the structure of an additional  $U(1)$  group in  $E_6$  theories [33] and  $G'_\phi$  is the Fermi constant associated with the new  $U(1)$  group [34]. Note that this contribution has the wrong sign to account for the large negative value of  $R_A^{T=1}$ .

Alternatively, one might consider new tree-level interactions generated by supersymmetric extensions of the SM. Such interactions arise when R-parity, or equivalently,  $B - L$ , is not conserved ( $B$  and  $L$  denote baryon and lepton number, respectively). The contribution from R-parity violating SUSY interactions is given by [35,34]

$$R_A^{T=1}(\text{new}) = -\Delta_{12k}(\tilde{e}_R^k) + \left( \frac{1}{1 - 4\sin^2 \theta_W} \right) [\Delta'_{11k}(\tilde{d}_R^k) - \Delta'_{1j1}(\tilde{q}_L^j)] \quad , \quad (61)$$

where

$$\Delta_{ijk}(\tilde{f}) = \frac{1}{4\sqrt{2}} \frac{|\lambda_{ijk}|^2}{G_\mu M_{\tilde{f}}^2} \quad , \quad (62)$$

with  $\tilde{f}$  denoting the superpartner of fermion  $f$  and  $i, j, k$  label fermion generations. The terms having a prime are semileptonic whereas the un-primed terms are purely leptonic. In principle, the correction in Eq. (61) could generate a negative contribution to  $R_A^{T=1}$ . However, the various other electroweak data constrain the terms appearing in this expression. For example, relations between  $G_\mu$  and other SM parameters require

$$-0.0023 \leq \Delta_{12k}(\tilde{e}_R^k) \leq 0.0028 \quad , \quad (63)$$

at 90 % C.L., so that the first term in Eq. (61) cannot provide the large negative contribution needed to explain the SAMPLE result. Similarly, assuming only the semileptonic R-parity violating interactions modify the weak charge of nuclei, the recent determination of the cesium weak charge by the Boulder group [36] implies that

$$0.0025 \leq 2.4\Delta'_{11k}(\tilde{d}_R^k) - 2.7\Delta'_{1j1}(\tilde{q}_L^j) \leq 0.015 \quad , \quad (64)$$

at 95 % C.L. (for  $m_H = 300$  GeV). Thus, it appears unlikely that the second term in Eq. (61) could enhance  $R_A^{T=1}$  by a factor of two.

In short, two of the most popular new physics scenarios having implications for low-energy phenomenology appear unlikely to enhance  $R_A^{T=1}$  significantly. Thus, if more conventional hadronic and nuclear processes cannot account for the SAMPLE result, one may be forced to consider more exotic alternatives.

## ACKNOWLEDGEMENT

We wish to thank D. Beck, E.J. Beise, and R. McKeown for useful discussions. This work was supported in part under U.S. Department of Energy contract #DE-AC05-84ER40150, the National Science Foundation and a National Science Foundation Young Investigator Award.

## REFERENCES

- [1] D.T. Spayde et al., the SAMPLE Collaboration, Phys. Rev. Lett. **84**, 1106 (2000).
- [2] M.J. Musolf et al., Phys. Reports 239, 1 (1994).
- [3] E. Caso et al., Particle Data Group, Euro. Phys. J. C 3, 1 (1998).
- [4] M. J. Musolf and B. R. Holstein, Phys. Lett. B 242, 461 (1990).
- [5] M. J. Musolf and B. R. Holstein, Phys. Rev. D 43, 2956 (1991).
- [6] E.J. Beise, talk given at Bates25 Symposium, Nov. 3-5, 1999, Cambridge, MA; D.H. Beck and R.D. McKeown, private communication.
- [7] W. C. Haxton, E. M. Henley and M. J. Musolf, Phys. Rev. Lett. 63, 949 (1989).
- [8] C. S. Wood et al., Science 275, 1759 (1997).
- [9] D. B. Kaplan and M. J. Savage, Nucl. Phys. A 556, 653 (1993); *Erratum-ibid.* A 570, 833 (1994); *Erratum-ibid.* A 580, 679 (1994).
- [10] E. Jenkins and A. V. Manohar, Phys. Lett. B 255, 558 (1991); B 259, 353 (1991).
- [11] Ulf-G. Meissner, Int. J. Mod. Phys. E 1, 561 (1992).
- [12] B.R. Holstein, *Weak Interactions in Nuclei*, World Scientific, 1989.
- [13] W. Haeberli and B.R. Holstein in *Symmetries and Fundamental Interactions in Nuclei*, W.C. Haxton and E.M. Henley, Eds., World Scientific, Singapore, 1995, p. 17.
- [14] B. Desplanques, J. F. Donoghue and B. R. Holstein, Ann. Phys. 124, 449 (1980).
- [15] T. R. Hemmert, B. R. Holstein and J. Kambor, J. Phys. G 24, 1831 (1998).
- [16] B. J. Bjorken and S. Drell, *Relativistic Quantum Fields*, McGraw-Hill, New York, 1965.
- [17] E. G. Adelberger and W. C. Haxton, Ann. Rev. Nucl. Part. Sci. 35, 501 (1985).
- [18] N. Kaiser and Ulf.-G. Meissner, Nucl. Phys. A 499, 699 (1989); *ibid.* A 510, 759 (1990); Ulf.-G. Meissner and H. Weigel, Phys. Lett. B 447, 1 (1999).
- [19] E. M. Henley, W.-Y. P. Hwang and L. S. Kisslinger, Phys. Lett. B 367, 21 (1996); *Erratum-ibid.* B 440, 449 (1998).
- [20] E. Jenkins et al., Phys. Lett. B 302, 482 (1993); B 388, 866 (1996) [E].
- [21] Ulf-G. Meissner and S. Steininger, Nucl. Phys. B 499, 349 (1997).
- [22] L. Durand and P. Ha, Phys. Rev. D 58, 013010 (1998).
- [23] S. Puglia and M. J. Ramsey-Musolf, hep-ph/9911542.
- [24] Ulf.-G. Meissner and S. Steininger, Nucl. Phys. B 499, 349 (1997); Ulf.-G. Meissner, hep-ph/9709402.
- [25] G. Ecker, J. Gasser, A. Pich and E. de Rafael, Nucl. Phys. B 321, 311 (1989).
- [26] G. Höhler et al., Nucl. Phys. **B114**, 505 (1976).
- [27] G. B. Feldman et al., Phys. Rev. C 43, 863 (1991).
- [28] R. Balzer et al., Phys. Rev. C 30, 1409 (1984).
- [29] B. Desplanques, Nucl. Phys. A 335, 147 (1980).
- [30] S. Kistyrn et al., Phys. Rev. Lett. **58**, 1616 (1987).
- [31] J. J. Sakurai, *Currents and mesons*, the University of Chicago Press, 1969.
- [32] H.-W. Hammer and M.J. Ramsey-Musolf, Phys. Rev. C 60, 45205 (1999).
- [33] D. London and J.L. Rosner, Phys. Rev. **D 34**, 1530 (1986).
- [34] M.J. Ramsey-Musolf, Phys. Rev. **C 60**, 015501 (1999).
- [35] V. Barger, G.F. Guidice, T. Han, Phys. Rev. **D 40**, 2987 (1989).

[36] S.C. Bennett and C.E. Wieman, Phys. Rev. Lett. **82**, 2484 (1999); C.S. Wood *et al.*, Science **275**, 1759 (1997). For recent analyses of the theoretical implications of these measurements, see for example, R. Casalbuoni, S. De Curtis, D. Dominici, R. Gatto, S. Riemann, hep-ph/0001215.

## APPENDIX A: FORMALISM

In this section we first review the general parity and CP conserving Lagrangians including  $N, \pi, \Delta, \gamma$  in the relativistic form. We follow standard conventions and introduce

$$\Sigma = \xi^2, \quad \xi = e^{\frac{i\pi}{F_\pi}}, \quad \pi = \frac{1}{2}\pi^a \tau^a \quad (A1)$$

with  $F_\pi = 92.4$  MeV being the pion decay constant. The chiral vector and axial vector currents are given by

$$\begin{aligned} A_\mu &= -\frac{i}{2}(\xi D_\mu \xi^\dagger - \xi^\dagger D_\mu \xi) = -\frac{D_\mu \pi}{F_\pi} + O(\pi^3) \\ V_\mu &= \frac{1}{2}(\xi D_\mu \xi^\dagger + \xi^\dagger D_\mu \xi) \quad . \end{aligned} \quad (A2)$$

and we require also the gauge and chiral covariant derivatives

$$\begin{aligned} D_\mu \pi &= \partial_\mu \pi - ie\mathcal{A}_\mu [Q, \pi] \\ \mathcal{D}_\mu &= D_\mu + V_\mu \quad , \end{aligned} \quad (A3)$$

with

$$Q = \begin{pmatrix} \frac{2}{3} & 0 \\ 0 & -\frac{1}{3} \end{pmatrix} \quad (A4)$$

and  $\mathcal{A}_\mu$  being the photon field. The chiral field strength tensors are

$$F_{\mu\nu}^\pm = \frac{1}{2}(\partial_\mu \mathcal{A}_\nu - \partial_\nu \mathcal{A}_\mu)(\xi Q' \xi^\dagger \pm \xi^\dagger Q' \xi) \quad (A5)$$

with

$$Q' = \begin{pmatrix} 1 & 0 \\ 0 & 0 \end{pmatrix} \quad (A6)$$

acting in the space of baryon isodoublets.

For the moment, we restrict our attention to SU(2) flavor space and consider just  $\pi$ ,  $N$ , and  $\Delta$  degrees of freedom. We represent the nucleon as a two component isodoublet field, while for the  $\Delta$ , we use the isospurion formalism, treating the  $\Delta$  field  $T_\mu^i(x)$  as a vector spinor in both spin and isospin space [15] with the constraint  $\tau^i T_\mu^i(x) = 0$ . The components of this field are

$$T_\mu^3 = -\sqrt{\frac{2}{3}} \begin{pmatrix} \Delta^+ \\ \Delta^0 \end{pmatrix}_\mu, \quad T_\mu^+ = \begin{pmatrix} \Delta^{++} \\ \Delta^+/\sqrt{3} \end{pmatrix}_\mu, \quad T_\mu^- = -\begin{pmatrix} \Delta^0/\sqrt{3} \\ \Delta^- \end{pmatrix}_\mu. \quad (A7)$$

The field  $T_\mu^i$  also satisfies the constraints for the ordinary Schwinger-Rarita spin- $\frac{3}{2}$  field,

$$\gamma^\mu T_\mu^i = 0 \quad \text{and} \quad p^\mu T_\mu^i = 0 \quad . \quad (\text{A8})$$

We eventually convert to the heavy baryon expansion, in which case the latter constraint becomes  $v^\mu T_\mu^i = 0$  with  $v_\mu$  the heavy baryon velocity.

It is useful to review the spacetime and chiral transformation properties of the various fields. Under a chiral transformation,

$$\begin{aligned} \xi &\rightarrow L\xi U^\dagger = U\xi R^\dagger \\ A_\mu &\rightarrow U A_\mu U^\dagger \\ \mathcal{D}_\mu &\rightarrow U \mathcal{D}_\mu U^\dagger, \end{aligned} \quad (\text{A9})$$

and

$$N \rightarrow UN, \quad T_\mu \rightarrow UT_\mu, \quad \Sigma \rightarrow L\Sigma R^\dagger \quad \text{etc.} \quad (\text{A10})$$

In the  $SU(2)$  sector parity violating effects are conveniently described by introducing the operators [9]:

$$X_L^a = \xi^\dagger \tau^a \xi, \quad X_R^a = \xi \tau^a \xi^\dagger, \quad X_\pm^a = X_L^a \pm X_R^a \quad . \quad (\text{A11})$$

which transform as

$$X_{L,R}^a \rightarrow U X_{L,R}^a \tilde{U}^\dagger \quad , \quad (\text{A12})$$

with the index  $a$  rotating like a vector of  $SU(2)_L$  and  $SU(2)_R$  respectively.

The P and CP transformation properties of these fields are shown in Table 2.

Field	P	CP
$A_\mu$	$-A^\mu$	$-A_\mu^T$
$N$	$\gamma_0 N$	$\gamma_0 C \bar{N}^T$
$T_\mu$	$-\gamma_0 T^\mu$	$-\delta(a) \gamma_0 C \bar{T}_\mu^{Ta}$
$X_L^a$	$X_R^a$	$\delta(a) X_L^{Ta}$
$X_R^a$	$X_L^a$	$\delta(a) X_R^{Ta}$
$F_{\mu\nu}^\pm$	$\pm F^{\pm\mu\nu}$	$-F^{\pm T\mu\nu}$

TABLE II. Parity (P) and CP transformation properties of chiral fields. Here, T denotes the transpose, C is the charge conjugation matrix ( $C = i\gamma_2\gamma_0$  in the Dirac representation) and  $\delta(i) = 1, i = 1, 3$  and  $\delta(2) = -1$ .

Finally, we note that in the Lagrangians of Section III, one has the following definitions:

$$\begin{aligned} \mathcal{D}_\mu^{ij} &= \delta^{ij} \mathcal{D}_\mu - 2i\epsilon^{ijk} V_\mu^k \\ \omega_\mu^i &= Tr[\tau^i A_\mu] \\ A_\mu^{ij} &= \xi_{3/2}^{ik} A_\mu \xi_{3/2}^{kj} \quad , \end{aligned} \quad (\text{A13})$$

where  $\xi_{3/2}^{ij} = \frac{2}{3}\delta^{ij} - \frac{i}{3}\epsilon_{ijk}\tau^k$  is the isospin 3/2 projection operator.

## APPENDIX B: THE $SU(3)$ PARITY VIOLATING AND CP CONSERVING LAGRANGIAN

In this Appendix we list the parity violating and CP conserving  $SU(3)$  Lagrangian for the pseudoscalar meson octet and baryon octet. We are interested in the diagonal case of the parity violating electron nucleon scattering. Hence, we include only those interaction terms that ensure strangeness and charge conservation at each vertex. In the following we use  $\xi = e^{\frac{i\pi}{F\pi}}, \pi = \frac{1}{2}\pi^a\lambda^a, X_L^a = \xi^\dagger\lambda^a\xi, X_R^a = \xi\lambda^a\xi^\dagger, X_\pm^a = X_L^a \pm X_R^a, [A, B]_\pm = AB \pm BA$ .

We classify the parity violating Lagrangian according to isospin violation  $\Delta T = 0, 1, 2$ , which arises from the operators of  $X_L^a, X_R^a$ , their combinations and products. The  $\Delta T = 2$  piece comes from the operators  $\mathcal{I}^{ab}\{X_L^a\mathcal{O}X_L^b \pm (L \leftrightarrow R)\}$  with  $\mathcal{O} = N, \bar{N}, A_\mu$  and

$$\mathcal{I}^{ab} = \frac{1}{3} \begin{pmatrix} 1 & 0 & 0 \\ 0 & 1 & 0 \\ 0 & 0 & -2 \end{pmatrix} , \quad (B1)$$

where  $a, b = 1, 2, 3$ . Several operators contribute to the  $\Delta T = 1$  part, like  $X_\pm^3, f^{3ab}\{X_L^a\mathcal{O}X_L^b \pm (L \leftrightarrow R)\}, d^{3ab}\{X_L^a\mathcal{O}X_L^b \pm (L \leftrightarrow R)\}$  where  $f^{abc}, d^{abc}$  are the antisymmetric and symmetric structure constants of  $SU(3)$  algebra. With the requirement that the final Lagrangian be hermitian, parity-violating and CP-conserving, the operator with  $f^{3ab}$  vanishes. For the  $\Delta T = 0$  part relevant operators are  $\mathbf{1}, X_\pm^8, f^{8ab}\{X_L^a\mathcal{O}X_L^b \pm (L \leftrightarrow R)\}, d^{8ab}\{X_L^a\mathcal{O}X_L^b \pm (L \leftrightarrow R)\}, \delta^{ab}\{X_L^a\mathcal{O}X_L^b \pm (L \leftrightarrow R)\}$ . For the same reason the  $f^{8ab}$  structure does not contribute. Note the matrix identity  $\lambda^a\lambda^b\lambda^a = 4(C_2(\mathbf{3}) - \frac{1}{2}C_2(\mathbf{8}))\lambda^b$ , where  $C_2(\mathbf{3}), C_2(\mathbf{8})$  are the Casimir invariants of the basic and adjoint representations of  $SU(3)$  group respectively. Hence, the operator containing  $\delta^{ab}$  is identical to the unit operator.

Based on these considerations, we obtain

$$\begin{aligned} \mathcal{L}_{\Delta T=0}^{\text{PV}} = & h_3 F_\pi \text{Tr} \bar{N}[X_-^8, N]_+ + h_4 F_\pi \text{Tr} \bar{N}[X_-^8, N]_- + v_1 \text{Tr} \bar{N}\gamma^\mu [A_\mu, N]_+ \\ & + v_2 \text{Tr} \bar{N}\gamma^\mu [A_\mu, N]_- + \frac{v_7}{2} \text{Tr} \bar{N}\gamma^\mu A_\mu N X_+^8 + \frac{v_8}{2} \text{Tr} \bar{N}\gamma^\mu X_+^8 N A_\mu \\ & + \frac{v_9}{2} \text{Tr} \bar{N}\gamma^\mu [X_+^8, A_\mu]_+ N + \frac{v_{10}}{2} \text{Tr} \bar{N}\gamma^\mu N [X_+^8, A_\mu]_+ + a_5 \text{Tr} \bar{N}\gamma^\mu \gamma_5 A_\mu N X_-^8 \\ & + a_6 \text{Tr} \bar{N}\gamma^\mu \gamma_5 X_-^8 N A_\mu + a_7 \text{Tr} \bar{N}\gamma^\mu \gamma_5 [X_-^8, A_\mu]_+ N + a_8 \text{Tr} \bar{N}\gamma^\mu \gamma_5 N [X_-^8, A_\mu]_+ \\ & + \sqrt{3}v_{11} d^{8ab} \text{Tr} \{ \bar{N}\gamma^\mu N X_L^a A_\mu X_L^b + (L \leftrightarrow R) \} \\ & + \sqrt{3}v_{12} d^{8ab} \text{Tr} \{ \bar{N}\gamma^\mu X_L^a A_\mu X_L^b N + (L \leftrightarrow R) \} \\ & + \sqrt{3}v_{13} d^{8ab} \text{Tr} \{ \bar{N}\gamma^\mu X_L^a N [X_L^b, A_\mu]_+ + (L \leftrightarrow R) \} \\ & + \sqrt{3}v_{14} d^{8ab} \text{Tr} \{ \bar{N}\gamma^\mu [X_L^a, A_\mu]_+ N X_L^b + (L \leftrightarrow R) \} \\ & + \sqrt{3}a_9 d^{8ab} \text{Tr} \{ \bar{N}\gamma^\mu \gamma_5 N X_L^a A_\mu X_L^b - (L \leftrightarrow R) \} \\ & + \sqrt{3}a_{10} d^{8ab} \text{Tr} \{ \bar{N}\gamma^\mu \gamma_5 X_L^a A_\mu X_L^b N - (L \leftrightarrow R) \} \\ & + \sqrt{3}a_{11} d^{8ab} \text{Tr} \{ \bar{N}\gamma^\mu \gamma_5 X_L^a N [X_L^b, A_\mu]_+ - (L \leftrightarrow R) \} \\ & + \sqrt{3}a_{12} d^{8ab} \text{Tr} \{ \bar{N}\gamma^\mu \gamma_5 [X_L^a, A_\mu]_+ N X_L^b - (L \leftrightarrow R) \} , \end{aligned} \quad (B2)$$

$$\begin{aligned}
\mathcal{L}_{\Delta T=1}^{\text{PV}} = & h_1 F_\pi \text{Tr} \bar{N} [X_-^3, N]_+ + h_2 F_\pi \text{Tr} \bar{N} [X_-^3, N]_- + \frac{v_3}{2} \text{Tr} \bar{N} \gamma^\mu A_\mu N X_+^3 \\
& + \frac{v_4}{2} \text{Tr} \bar{N} \gamma^\mu X_+^3 N A_\mu + \frac{v_5}{2} \text{Tr} \bar{N} \gamma^\mu [X_+^3, A_\mu]_+ N + \frac{v_6}{2} \text{Tr} \bar{N} \gamma^\mu N [X_+^3, A_\mu]_+ \\
& + a_1 \text{Tr} \bar{N} \gamma^\mu \gamma_5 A_\mu N X_-^3 + a_2 \text{Tr} \bar{N} \gamma^\mu \gamma_5 X_-^3 N A_\mu + a_3 \text{Tr} \bar{N} \gamma^\mu \gamma_5 [X_-^3, A_\mu]_+ N \\
& + a_4 \text{Tr} \bar{N} \gamma^\mu \gamma_5 N [X_-^3, A_\mu]_+ + v_{15} d^{3ab} \text{Tr} \{ \bar{N} \gamma^\mu N X_L^a A_\mu X_L^b + (L \leftrightarrow R) \} \\
& \quad + v_{16} d^{3ab} \text{Tr} \{ \bar{N} \gamma^\mu X_L^a A_\mu X_L^b N + (L \leftrightarrow R) \} \\
& \quad + v_{17} d^{3ab} \text{Tr} \{ \bar{N} \gamma^\mu X_L^a N [X_L^b, A_\mu]_+ + (L \leftrightarrow R) \} \\
& \quad + v_{18} d^{3ab} \text{Tr} \{ \bar{N} \gamma^\mu [X_L^a, A_\mu]_+ N X_L^b + (L \leftrightarrow R) \} \\
& \quad + a_{13} d^{3ab} \text{Tr} \{ \bar{N} \gamma^\mu \gamma_5 N X_L^a A_\mu X_L^b - (L \leftrightarrow R) \} \\
& \quad + a_{14} d^{3ab} \text{Tr} \{ \bar{N} \gamma^\mu \gamma_5 X_L^a A_\mu X_L^b N - (L \leftrightarrow R) \} \\
& \quad + a_{15} d^{3ab} \text{Tr} \{ \bar{N} \gamma^\mu \gamma_5 X_L^a N [X_L^b, A_\mu]_+ - (L \leftrightarrow R) \} \\
& \quad + a_{16} d^{3ab} \text{Tr} \{ \bar{N} \gamma^\mu \gamma_5 [X_L^a, A_\mu]_+ N X_L^b - (L \leftrightarrow R) \} , \quad (B3)
\end{aligned}$$

$$\begin{aligned}
\mathcal{L}_{\Delta T=2}^{\text{PV}} = & \frac{v_{19}}{2} \mathcal{I}^{ab} \text{Tr} \{ \bar{N} \gamma^\mu N X_L^a A_\mu X_L^b + (L \leftrightarrow R) \} \\
& + \frac{v_{20}}{2} \mathcal{I}^{ab} \text{Tr} \{ \bar{N} \gamma^\mu X_L^a A_\mu X_L^b N + (L \leftrightarrow R) \} \\
& + \frac{v_{21}}{2} \mathcal{I}^{ab} \text{Tr} \{ \bar{N} \gamma^\mu X_L^a N [X_L^b, A_\mu]_+ + (L \leftrightarrow R) \} \\
& + \frac{v_{22}}{2} \mathcal{I}^{ab} \text{Tr} \{ \bar{N} \gamma^\mu [X_L^a, A_\mu]_+ N X_L^b + (L \leftrightarrow R) \} \\
& + \frac{a_{17}}{2} \mathcal{I}^{ab} \text{Tr} \{ \bar{N} \gamma^\mu \gamma_5 N X_L^a A_\mu X_L^b - (L \leftrightarrow R) \} \\
& + \frac{a_{18}}{2} \mathcal{I}^{ab} \text{Tr} \{ \bar{N} \gamma^\mu \gamma_5 X_L^a A_\mu X_L^b N - (L \leftrightarrow R) \} \\
& + \frac{a_{19}}{2} \mathcal{I}^{ab} \text{Tr} \{ \bar{N} \gamma^\mu \gamma_5 X_L^a N [X_L^b, A_\mu]_+ - (L \leftrightarrow R) \} \\
& + \frac{a_{20}}{2} \mathcal{I}^{ab} \text{Tr} \{ \bar{N} \gamma^\mu \gamma_5 [X_L^a, A_\mu]_+ N X_L^b - (L \leftrightarrow R) \} . \quad (B4)
\end{aligned}$$

These Lagrangians contain 4 Yukawa couplings, 20 axial vector couplings and 22 vector couplings, all of which should be fixed from the experimental data or from model calculations. In reality, however, we have only limited information which constrains a few of them. It is useful to expand the above Lagrangians to the order involving the minimum number of Goldstone bosons and to collect those vertices needed in the calculation of  $R_A$ :

$$\begin{aligned}
\mathcal{L}_{Yukawa}^{1\pi} = & 2\sqrt{2}i(h_1 + h_2)(\bar{p}n\pi^+ - \bar{n}p\pi^-) \\
& + i[h_1 - h_2 + \sqrt{3}(h_3 - h_4)](\bar{p}\Sigma^0 K^+ - \bar{\Sigma}^0 pK^-) \\
& + \sqrt{2}i[h_1 - h_2 + \sqrt{3}(h_3 - h_4)](\bar{n}\Sigma^- K^+ - \bar{\Sigma}^- nK^-) \\
& - i[\frac{h_1}{\sqrt{3}} + \sqrt{3}h_2 + h_3 + 3h_4](\bar{p}\Lambda K^+ - \bar{\Lambda}pK^-) + \dots . \quad (B5)
\end{aligned}$$

$$\mathcal{L}_V^{1\pi} = -\frac{h_V^{pn\pi^+}}{F_\pi} \bar{p} \gamma^\mu n D_\mu \pi^+ - \frac{h_V^{p\Sigma^0 K^+}}{F_\pi} \bar{p} \gamma^\mu \Sigma^0 D_\mu K^+$$

$$-\frac{h_V^{n\Sigma^-K^+}}{F_\pi}\bar{n}\gamma^\mu\Sigma^-D_\mu K^+ - \frac{h_V^{p\Lambda K^+}}{F_\pi}\bar{p}\gamma^\mu\Lambda D_\mu K^+ + h.c. + \dots, \quad (B6)$$

where

$$\begin{aligned} h_V^{pn\pi^+} &= \frac{v_1+v_2}{\sqrt{2}} + \frac{4\sqrt{2}}{3}(v_{14}-v_{12}) + \frac{\sqrt{6}}{3}(v_7+v_9) + \frac{\sqrt{2}}{3}v_{20} \\ h_V^{p\Sigma^0K^+} &= \frac{1}{2}(v_1-v_2+v_4+v_6) + \frac{v_8-v_{10}}{2\sqrt{3}} + \frac{2}{3}(v_{11}-v_{13}-v_{15}-v_{21}-\frac{1}{2}v_{17}) + 2v_{18} \\ h_V^{n\Sigma^-K^+} &= \frac{1}{\sqrt{2}}(v_1-v_2+v_6-v_4) + \frac{1}{\sqrt{6}}(v_8-v_{10}) + \frac{\sqrt{2}}{3}(v_{17}+v_{21}) + \frac{2\sqrt{2}}{3}(v_{11}-v_{13}-v_{15}) \\ h_V^{p\Lambda K^+} &= \frac{1}{\sqrt{3}}\left(-\frac{v_1}{2} + \frac{2}{3}v_{11} - \frac{4}{3}v_{12} + \frac{16}{3}v_{13} - \frac{2}{3}v_{14} - \frac{2}{3}v_{15} + \frac{4}{3}v_{16} - \frac{17}{3}v_{17}\right. \\ &\quad \left.+ \frac{4}{3}v_{18} - \frac{3}{2}v_2 + \frac{v_4}{2} - v_5 + \frac{v_6}{2}\right) + \frac{v_8-v_{10}}{6} + \frac{2v_7+v_9}{3} \end{aligned} \quad . \quad (B7)$$

$$\begin{aligned} \mathcal{L}_A^{2\pi} &= -i\frac{h_A^{p\pi}}{f_\pi^2}\bar{p}\gamma^\mu\gamma_5 p(\pi^+D_\mu\pi^- - \pi^-D_\mu\pi^+) \\ &\quad -i\frac{h_A^{pK}}{f_\pi^2}\bar{p}\gamma^\mu\gamma_5 p(K^+D_\mu K^- - K^-D_\mu K^+) \\ &\quad -i\frac{h_A^{n\pi}}{f_\pi^2}\bar{n}\gamma^\mu\gamma_5 n(\pi^+D_\mu\pi^- - \pi^-D_\mu\pi^+) \\ &\quad -i\frac{h_A^{nK}}{f_\pi^2}\bar{n}\gamma^\mu\gamma_5 n(K^+D_\mu K^- - K^-D_\mu K^+) + \dots, \end{aligned} \quad (B8)$$

where

$$\begin{aligned} h_A^{p\pi} &= 2a_3 - \frac{4}{3}a_{16} + \frac{2}{3}a_{14} - a_{18} + 2a_{13} \\ h_A^{pK} &= a_3 - a_4 + \sqrt{3}(a_7 - a_8) + a_9 + a_{10} + a_{11} + a_{12} + \frac{1}{3}(a_{16} + a_{14} - a_{18} + a_{13} - a_{19}) \\ h_A^{n\pi} &= 2a_3 - \frac{4}{3}a_{16} + \frac{2}{3}a_{14} + a_{18} + 2a_{13} \\ h_A^{nK} &= a_4 + \sqrt{3}a_8 + a_9 + \frac{5}{2}a_{10} - 2a_{11} - a_{15} + a_{14} + \frac{1}{3}(a_{18} + a_{19} + a_{13}) \end{aligned} \quad (B9)$$

Note only  $a_{18}$  contributes to  $R_A$  in the parity violating two pions vertices. In the two kaons vertices  $a_{3-4}, a_{7-8}, a_{10-19}$  all lead to nonzero contribution to  $R_A$ .

## APPENDIX C: $\Delta$ INTERMEDIATE STATES AND EM INSERTIONS

As noted in Section IV, the amplitudes of Figures 4-6 vanish through  $\mathcal{O}(1/\Lambda_\chi^2)$ . Below, we briefly summarize the reasons behind this result.

### 1. PV $\pi\Delta N$ contribution

In the case where the  $\Delta$  enters as an intermediate state we have the Feynman diagrams shown in Figure 4. Since the final and initial states are both nucleons, the two-pion parity

violating vertices in Eqs. (22)-(24) arise first at two-loop order and contribute to the nucleon anapole moment at the order of  $\mathcal{O}(1/\Lambda_\chi^3)$ . Although the PV  $N\Delta\pi$  interactions nominally contribute at lower order, in this case such contributions vanish up to  $\mathcal{O}(1/\Lambda_\chi^2)$ . The reason is as follows. Each of the parity violating and CP conserving single pion vertices has the same Lorentz structure— $i\gamma_5$ . In the heavy baryon expansion, the relevant vertices are obtained by the substitution  $P_+i\gamma_5P_+$ , which vanishes. The leading nonzero contribution arises at first order in the  $1/m_N$  expansion. Consequently, its contribution to the nucleon anapole moment appears only at  $\mathcal{O}(1/\Lambda_\chi^2 m_N)$ , and since in this work we truncate at  $\mathcal{O}(1/\Lambda_\chi^2)$ , the PV  $\pi\Delta N$  vertices do not contribute.

## 2. Magnetic moment insertions

The nucleon has a large isovector magnetic moment. We thus consider associated possible PV chiral loop corrections which lead to a nucleon anapole moment. The relevant diagrams are shown in Figure 5. At  $\mathcal{O}(1/\Lambda_\chi^2)$  there are only four relevant diagrams Figures 5a-d. Since the magnetic moment is of  $\mathcal{O}(1/\Lambda_\chi)$  and the strong pion baryon vertex is of  $\mathcal{O}(1/F_\pi)$ , the remaining PV vertex must be a Yukawa coupling if the loop is to contribute at  $\mathcal{O}(1/\Lambda_\chi^2)$  or lower. For the nucleon magnetic moment insertion we have, for example,

$$iM_{5a} + iM_{5b} = i\epsilon^{\mu\nu\alpha\beta}\varepsilon_\mu q_\nu v_\alpha \frac{\sqrt{2}g_A e \mu_N h_{\pi N}}{m_N F_\pi} [S_\beta, S_\sigma]_+ \int \frac{d^D k}{(2\pi)^D} \frac{k^\sigma}{v \cdot k} \frac{1}{v \cdot (q+k)} \frac{1}{k^2 - m_\pi^2 + i\epsilon}, \quad (C1)$$

where  $e_\mu$  is the photon polarization vector and  $\mu_N$  is the nucleon magnetic moment. The denominator of the integrand in (C1) is nearly the same as for  $M_{3e}$ . The numerator contains a single factor of  $S \cdot k$ . Hence, Figures 5a and 5b vanish for the same reason as does  $M_{3e}$ .

For the nucleon delta transition magnetic moment insertion we have

$$iM_{5c} + iM_{5d} = -\frac{2}{\sqrt{3}} \frac{g_{\pi N\Delta} e \mu_{\Delta N} h_{\pi N}}{m_N F_\pi} (q_\sigma \epsilon_\nu - \epsilon_\sigma q_\nu) [P_{3/2}^{\mu\nu} S^\sigma + S^\sigma P_{3/2}^{\nu\mu}] \times \int \frac{d^D k}{(2\pi)^D} \frac{k_\mu}{v \cdot k} \frac{1}{v \cdot (q+k)} \frac{1}{k^2 - m_\pi^2 + i\epsilon}, \quad (C2)$$

where  $\mu_{\Delta N}$  is the nucleon delta transition magnetic moment and  $P_{3/2}^{\mu\nu} = g^{\mu\nu} - v^\mu v^\nu + \frac{4}{3} S^\mu S^\nu$  is the spin  $\frac{3}{2}$  projection operator in the heavy baryon chiral perturbation framework. Since the integrand is the same as in  $M_{3e}$  the integral is proportional to  $v_\mu$ . Moreover,  $v_\mu P_{3/2}^{\mu\nu} = 0$ , so that  $M_{5c} + M_{5d} = 0$ . Finally, the  $\Delta$  magnetic insertions of Figures 5e-h require the PV  $N\Delta\pi$  vertex, which starts off at  $\mathcal{O}(1/m_N F_\pi)$ . Thus, the latter do not contribute up to  $\mathcal{O}(1/\Lambda_\chi^2)$ . In short, none of the magnetic insertions contribute at the order to which we work in this analysis.

### 3. PV electromagnetic insertions

Another possible source to the nucleon anapole moment arises from the PV magnetic moment like insertions as shown in Figure 6. All three PV  $\gamma NN$  vertices  $c_{1-3}$  in Eq. (21) and PV  $\gamma\Delta N$  vertices  $d_{4-6}$  in Eq. (25) start off with one pion, so they are of order  $\mathcal{O}(1/\Lambda_\chi F_\pi)$ . Vertices  $d_{7,8}$  have two pions and are order  $\mathcal{O}(1/\Lambda_\chi F_\pi^2)$ . The corresponding contributions to the nucleon anapole moment appear at order of  $\mathcal{O}(1/\Lambda_\chi^3)$  or  $\mathcal{O}(1/\Lambda_\chi^4)$ , respectively. The leading PV  $\gamma\Delta N$  vertices  $d_{1-3}$  do not have pions and are of the order  $\mathcal{O}(1/\Lambda_\chi)$ . In our case, however, the final and initial states are both nucleons. The  $\Delta$  can appear as the intermediate state inside the chiral loop, which leads to an additional factor  $1/F_\pi^2$  from two strong vertices. In the end  $d_{1-3}$  contributes to the nucleon anapole moment at  $\mathcal{O}(1/\Lambda_\chi^3)$ . Finally, the PV  $\gamma\Delta\Delta$  vertices contain one  $\pi$ . Since the  $\Delta$  can only appear as an intermediate state, this vertex contributes at two-loop order and is of higher-order in chiral counting than we consider here (the corresponding diagrams are not shown). Thus, to  $\mathcal{O}(1/\Lambda_\chi^2)$ , the PV electromagnetic insertions do not contribute.

## Figure Captions

FIG 1. Axial vector  $\gamma NN$  coupling, generated by PV hadronic interactions

Figure 2. Feynman diagrams for polarized electron nucleon scattering. Figure 2a gives tree-level  $Z^0$ -exchange amplitude, while FIG. 2b gives the anapole moment contribution. The dark circle indicates an axial vector coupling.

Figure 3. Meson-nucleon intermediate state contributions to the nucleon anapole moment. The shaded circle denotes the PV vertex. The solid, dashed and curly lines correspond to the nucleon, pion and photon respectively. For the  $SU(3)$  case the intermediate states can also be hyperons and kaons.

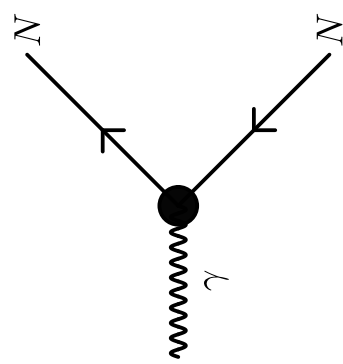
Figure 4. The contribution to the nucleon anapole moment from PV  $\pi\Delta N$  vertices. The double line is the  $\Delta$  intermediate state.

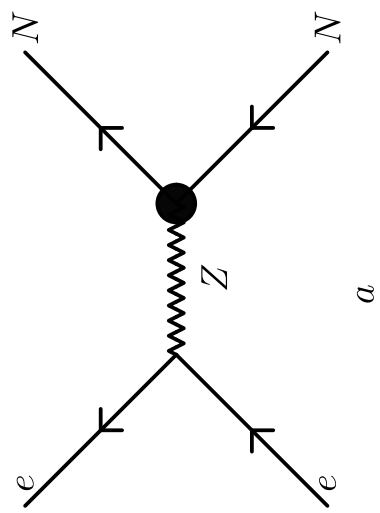
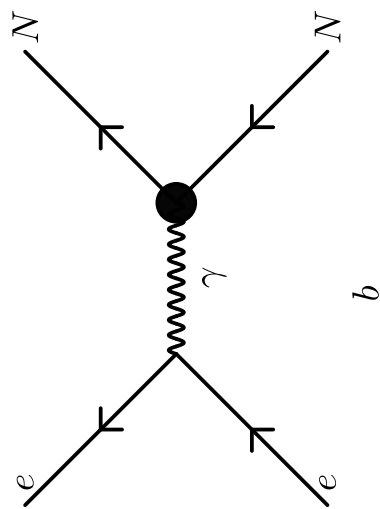
Figure 5. Anapole moment contributions generated by insertions of the baryon magnetic moment operator, denoted by the cross, and the PV hadronic couplings, denoted by the shaded circle.

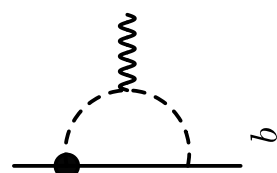
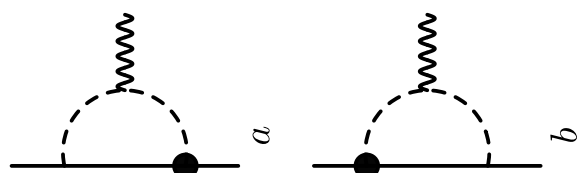
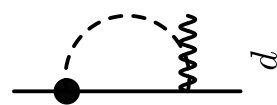
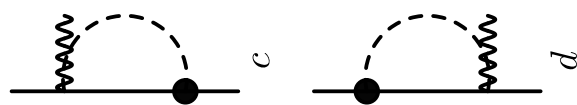
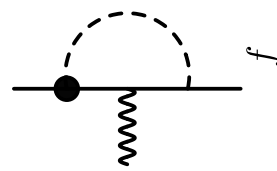
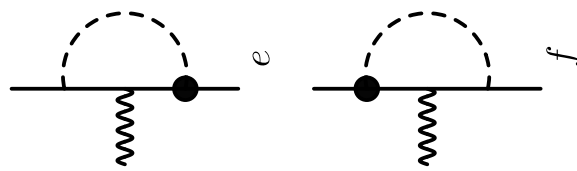
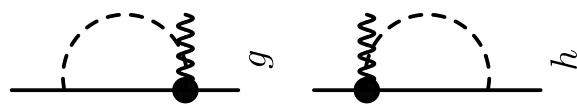
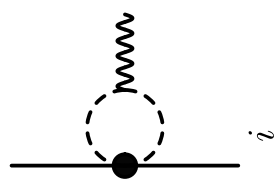
Figure 6. PV electromagnetic insertions, denoted by the overlapping cross and shaded circle.

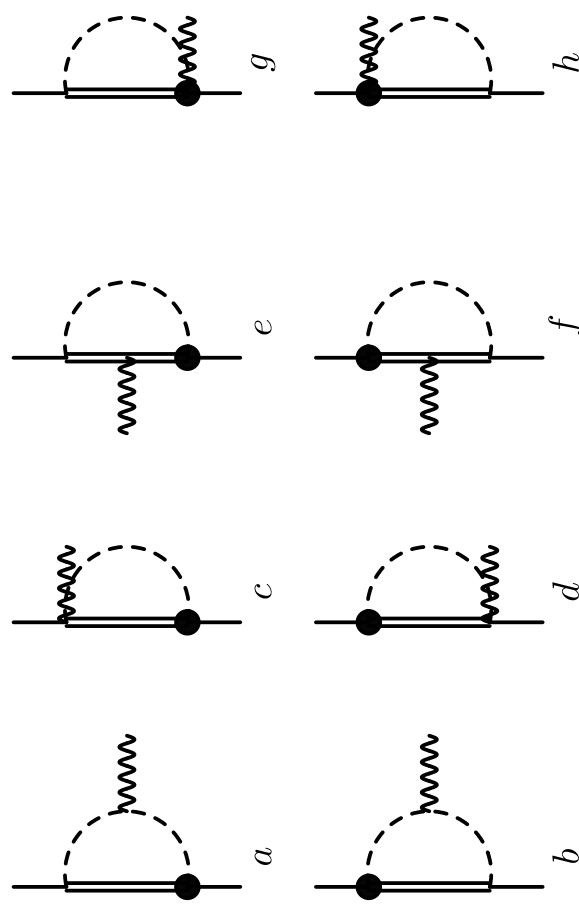
Figure 7. Vector meson contribution to the anapole moment. Shaded circle indicates PV hadronic coupling.

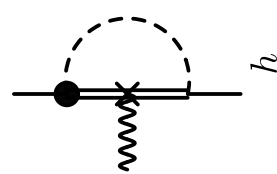
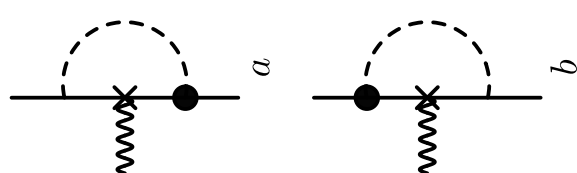
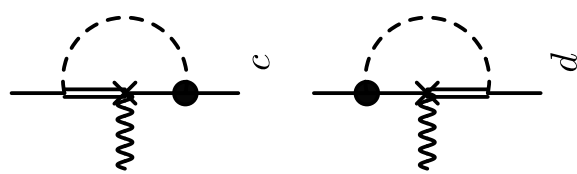
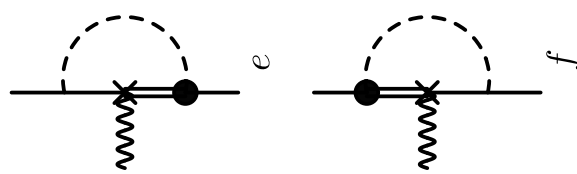
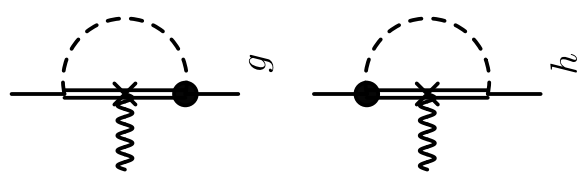
Figure 8. Contributions to (a) PV NN interaction and (b) PV two-body current generated by the vector terms in Eqs. (18-20).







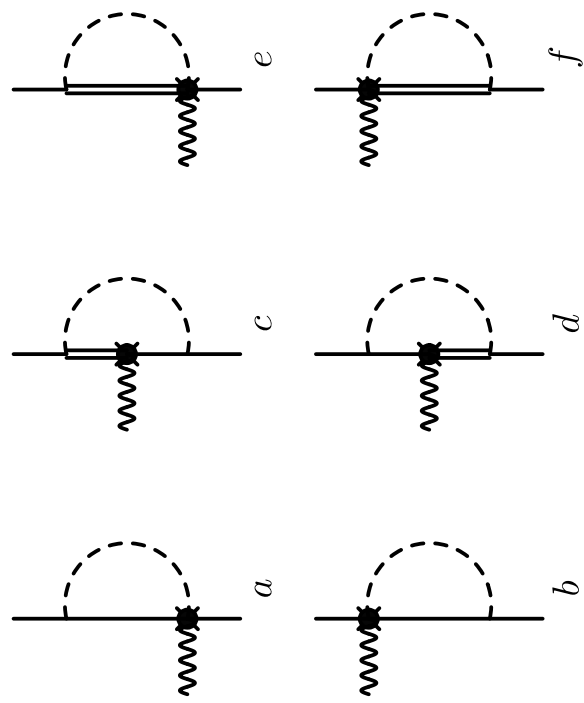


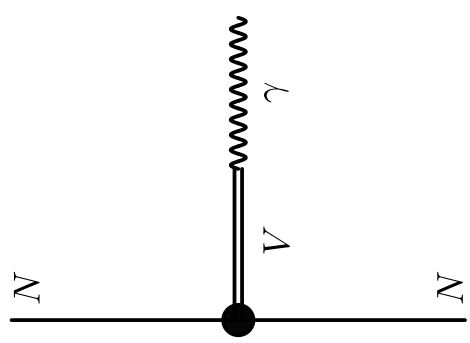


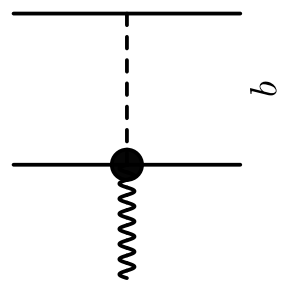
*f*

*d*

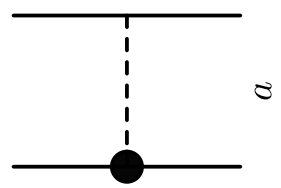
*b*







*b*



*a*